

WYOMING STATE GEOLOGICAL SURVEY

P.O. BOX 1347, LARAMIE, WY 82073

307-766-2286 • 307-766-2605 (fax)

wsgs.info@wyo.gov • www.wsgs.uwyo.edu

Director & State Geologist

Thomas A. Drean

Preliminary Geologic Map of the Dale Creek Quadrangle Albany County, Wyoming

by

Jacob D. Carnes, Ranie M. Lynds, Robert W. Gregory, and
Alan J. Ver Ploeg



Open File Report 13-2

Laramie, Wyoming

September 13, 2013

Prepared in cooperation with and research supported by the U.S. Geological Survey, National Cooperative Geologic Mapping Program, under USGS award number G12AC20466. The views and conclusions contained in this document are those of the authors and should not be interpreted as necessarily representing the official policies, either expressed or implied, of the U.S. Government.

This report is preliminary and has not been reviewed for conformity with Wyoming State Geological Survey editorial standards or with the North American Stratigraphic Code.

Contents

Introduction	2
Location	2
Geologic Setting.....	2
Structure.....	4
Economics	4
Geochemical Analyses.....	5
Description of Map Units.....	5
Quaternary Surficial Deposits	5
Holocene Alluvium (Qa)	5
Holocene and Pleistocene Mixed Alluvium and Colluvium (Qac).....	5
Paleozoic Sedimentary Rocks	5
Pennsylvanian Fountain Formation (Pf)	5
Middle Proterozoic Intrusive Igneous Rocks	6
Middle Proterozoic Lincoln Granite (Yln).....	6
Middle Proterozoic Monzodiorite (Ym) and Mafic Dikes (Ymd).....	6
Middle Proterozoic Porphyritic Granite (Yp)	7
Middle Proterozoic Sherman Granite (Ys).....	7
Middle Proterozoic Sherman Granite Inner Cap Rock Phase (Ysi)	9
Middle Proterozoic Sherman Granite Outer Cap Rock Phase (Yso)	9
Early Proterozoic Metamorphic Rocks.....	9
Early Proterozoic Biotite Gneiss (Xbg).....	9
References.....	10
Figures and Tables	13
Appendix	28

INTRODUCTION

The Dale Creek quadrangle is located in southeast Wyoming, on the southern boundary of the Laramie basin. Previous work in the area identified the the Middle Proterozoic Sherman batholith, Early Proterozoic metamorphic country rock, the northern portion of the Virginia Dale intrusion, Devonian kimberlites, and Pennsylvanian sediments. This study additionally identified multiple phases of the Sherman batholith including Lincoln Granite, porphyritic granite, and mafic bodies which have not previously been mapped in detail, as well as the inner and outer cap rock phases that have been described in Colorado relative to the Virginia Dale intrusion. Although Early Proterozoic metamorphic country rocks associated with the Cheyenne Shear Zone (CSZ) have been mapped to the south in Colorado, this is the first detailed investigation of these rocks in Wyoming. The emplacement of the Sherman batholith largely removed evidence of the CSZ in southeastern Wyoming. This map of the Dale Creek quadrangle aids in defining the original tectonic and stratigraphic conditions adjacent to the southern extent of the Wyoming Craton. Mapping was completed in cooperation with the U.S. Geological Survey 2012 STATEMAP grant award G12AC20466.

Initial mapping of the Dale Creek quadrangle was undertaken for the Laramie 1:100,000 scale map by Ver Ploeg (1999) and Ver Ploeg and Boyd (2007). Much of their work was based on previous work by Egler (1968) and Hausel and others (1979).

We wish to acknowledge and thank the landowners and caretakers for access to their private lands. This project would not have been possible without their generosity.

LOCATION

The Dale Creek 1:24,000 quadrangle is located along the southern boundary of Albany County, Wyoming, in Townships 12 and 13 north, and Ranges 71 and 72 west. The quadrangle is accessible along U.S. Highway 287 approximately 28.2 km (17.5 mi) south of Laramie, Wyoming, to the Wyoming–Colorado state line. Albany County Roads 222, 231, and 241 provide access to the quadrangle east of U.S. Highway 287. Access to the quadrangle is also possible from Albany County Road 234, which intersects Interstate 80, approximately 26.6 km (16.5 mi) east of Laramie. As much of the area covered by the Dale Creek 1:24,000 quadrangle is on private land, permission from the land owner must be obtained before entering private lands.

GEOLOGIC SETTING

The Dale Creek 1:24,000 quadrangle is located over the southern portion of the Middle Proterozoic Sherman batholith, including the northern margin of the Virginia Dale intrusive complex. The Sherman batholith was emplaced during a phase of anorogenic magmatism at 1.43 Ga, that included the emplacement of the Laramie Anorthosite Complex to the north (Aleinkoff, 1983; Frost and

others, 1990). The Sherman batholith cuts Archean crustal rocks of the Wyoming Province north of the CSZ (Frost and others, 1999), and Early Proterozoic metaigneous and metasedimentary rocks of the Colorado Province south of the CSZ. The metamorphic rocks south of the CSZ formed in relation to subduction and arc-magmatism at the southern margin of the Wyoming Province (DePaolo, 1981; Reed and others 1987). A 1.77 Ga biotite gneiss in the southeastern corner of the quadrangle represents the Colorado Province country rock.

The Sherman batholith is comprised of the Sherman Granite, Lincoln Granite, porphyritic granite, and mafic rocks, including pods and dikes of monzodiorite and diabase. Minor sodic rocks are also present within the Sherman batholith, but only isolated occurrences were observed within the Dale Creek 1:24,000 quadrangle. While essentially contemporaneous, the Sherman and Lincoln Granites are not genetically related products of fractionation of a single parental magma, but rather are the products of separate magmas derived from compositionally distinct sources (Edwards and Frost, 2000). The parental magma of the Sherman Granite resulted from the partial melting of iron-rich mafic rocks from the upper mantle; the Lincoln Granite parental magma was likely the product of partial melting and subsequent mixing of metapelitic crust and granodioritic or tonalitic crust (Edwards and Frost, 2000). The porphyritic granite is the product of mixing of the iron-rich, mantle-derived magma parental to the Sherman Granite, and the crustal-derived parental magmas of the Lincoln Granite. The emplacement of the Sherman Granite was preceded by the emplacement of sodic granitic rocks (Frost and others, 1999), sourced from partial melting of metabasalt (Edwards and Frost, 2000). Sodic rocks recognized within the Sherman batholith include the foliated Pole Mountain Gneiss (Harrison, 1951), which comprises most of the crest of the Sherman Mountains, and a non-foliated quartz monzodiorite enclave within the Sherman Granite near the Interstate 80 summit, 17.5 km (10.9 mi) east of Laramie (Frost and others, 1999). While officially termed a gneiss, the Pole Mountain Gneiss exhibits no evidence of sub-solidus deformation, but is instead a granodiorite and quartz monzonite that exhibits magmatic foliation (Frost and others, 1999).

The Virginia Dale intrusive complex comprises the southernmost portion of the Sherman batholith, and consists of coarse-grained, porphyritic granite and quartz monzonite of the Sherman Granite, divided into the inner and outer cap rock phases (Eggler, 1968), as well as dioritic rocks (Vasek and Kolker, 1999). Rhythmic layering of dioritic and granitic rocks is present within the Virginia Dale complex, and generally dips inward at $<45^\circ$. The relatively shallow dips of the rhythmic layering within the Virginia Dale complex indicate that the complex was constructed in part by repeated pulses of mafic magma into a floored, crystallizing chamber of granitic magma (Vasek and Kolker, 1999).

The rocks of the Sherman batholith are cut by Devonian kimberlitic diatremes in the southern portion of the batholith in Wyoming and Colorado. The kimberlitic bodies are part of the State Line District kimberlites, a group of approximately 35 diamondiferous diatremes that straddle the Wyoming–Colorado state line in the vicinities of Tie Siding and Virginia Dale (McCallum and others, 1975; Hausel and others, 1979); other kimberlite diatremes have been recognized from Boulder, Colorado, to the Iron Mountain area of the Laramie Range, 64 km (40 mi) north of the Colorado–Wyoming border (McCallum and others, 1975). The diatremes generally have a circular

to elliptical surface expression (McCallum and others, 1975). In southernmost Wyoming, the longest dimension of elongate diatremes is generally oriented between 340° and 350°, which suggests that diatreme emplacement was controlled by the pervasive north-south joint-set present in the mapping area. The diatremes are composed of kimberlitic intrusive breccia. The breccia consists of a light to dark green matrix of serpentine, calcite, dolomite, phlogopite, chlorite, talc, hematite, and perovskite that hosts subrounded to angular clasts of Precambrian crystalline rocks, Lower Paleozoic sedimentary rocks, and nodules of mantle rocks. Kimberlites typically weather to a light blue-gray soil commonly called “blue ground.”

The Sherman batholith is in places overlain by Upper Paleozoic sedimentary rocks. The Pennsylvanian Fountain Formation is the only Paleozoic sedimentary unit present within the Dale Creek 1:24,000 quadrangle. The Fountain Formation is a conglomeratic, coarse- to fine-grained arkosic sandstone with minor limestone, silt, and shale beds (Ver Ploeg and others, 2011) that ranges in thickness from 3 to 150 m (9.8 to 492 ft) in southeastern Wyoming, thickens to the southwest (Nicoll, 1963), but is less than 30 m (100 ft) within the map area.

STRUCTURE

The dominant structure within the Dale Creek 1:24,000 quadrangle is a network of east-west-trending reverse faults. On the western edge of the map, the fault system places Lincoln Granite, monzodiorite, and Sherman Granite above the Fountain Formation (Fig. 1); in the central and eastern portions of the map, the fault system dominantly cuts Sherman Granite. On the foot-wall near the western edge of the map, the Fountain Formation has been folded into a broad, shallowly plunging syncline. Pervasive 340°–350° trending lineaments in the western half of the map, visible in aerial imagery, are interpreted to be fractures or, where offset is observable, right-lateral strike-slip faults. In places, these fractures and faults are intruded by granite, monzodiorite, and diabase dikes. Offset across these right-lateral faults is observable on the reverse faults, and at the contacts between Sherman Granite and porphyritic granite, and porphyritic granite and Lincoln Granite. Many of the north-northwest-trending fractures and faults can be traced for tens of kilometers to the north. Also present within the map area are east-southeast-trending fractures and faults, but they are less abundant than the north-northwest-trending features. Left-lateral movement on some of the east-southeast-trending features offsets some of the north-northwest-trending fractures, faults, and dikes. One broadly curved fault in the northwestern corner of the map area exhibits normal displacement, with the hanging wall to the east on the inside of a broad curve, and the foot-wall to the west.

ECONOMICS

Minor historic mining has occurred within the bounds of the Dale Creek 1:24,000 quadrangle. Most were small pegmatites primarily mined for feldspars. Adits exploring for copper and other metals exist on the western boundary of the map along the major east-west fault trend. Several diamond-bearing kimberlite diatremes of the State Line kimberlite district are present within the southeastern portion of the quadrangle (McCallum and others, 1975; Hausel and others, 1979).

More recent work by Sutherland and others (2013) documents significant concentrations of rare earth elements at a few sample locations within the quadrangle. Overall, the economic potential within the Dale Creek quadrangle is low, with the exception of small granite and decorative stone quarries.

GEOCHEMICAL ANALYSES

Ten samples collected during mapping were analyzed for major (Fig. 2, Table 1), minor (Table 2), and rare earth element (REE) (Fig. 3) concentrations at ALS Chemex of Reno, Nevada. Additional analyses of two samples of Sherman Granite from Sutherland and others (2013) are also summarized in Tables 1 and 2. The sample locations of all samples in Figures 2 and 3 and Tables 1 and 2 are noted on the accompanying map (with the exception of the two Sutherland and others, 2013, samples). REE concentrations have been normalized according to Masuda and others (1973).

DESCRIPTION OF MAP UNITS

Quaternary Surficial Deposits

Holocene Alluvium (Qa)

Alluvium in the map area consists of unconsolidated to poorly consolidated clay, silt, sand, gravel, cobbles, and boulders, mainly in flood plains and lower stream terraces. The alluvial material is derived from all local geologic units. Alluvium generally ranges from 0 to 8 m (25 ft) in thickness.

Holocene and Pleistocene Mixed Alluvium and Colluvium (Qac)

Mixed alluvium and colluvium in the map area consists of sand, silt, clay, and gravel deposited along intermittent streams. This unit includes slope wash and smaller alluvial fan deposits that coalesce with alluvium. Alluvial and colluvial deposits are approximately 0 to 8 m (25 ft) thick.

Paleozoic Sedimentary Rocks

Pennsylvanian Fountain Formation (P_f)

The Fountain Formation is comprised of coarse-grained pink to red to purple sandstone and arkose, with some conglomerates, fossiliferous limey sandstones, siltstones, shales, and thin limestone lenses. Blotchy pink-red iron staining is common on arkosic, resistant, ridge-forming portions of the formation. Thickness is variable within the Laramie Basin (up to 150 m; 500 ft), thickening toward the southwest, but is generally less than 30 m (100 ft) within the map area, representing the lowest part of the formation.

Middle Proterozoic Intrusive Igneous Rocks

Middle Proterozoic Lincoln Granite (Yln)

The Lincoln Granite (Fig. 4) is a medium- to fine-grained, equigranular, orange-red to orange-gray, biotite granite that crops out in horizontal to moderately dipping sheets that tend to cap resistant hills, domes, and high ridges above the Sherman Granite. Some Lincoln Granite occurs as dikes (Fig. 5) and small inclusions/enclaves in the adjacent Sherman Granite. Major phases include quartz, microcline, plagioclase, perthite, and biotite (Fig. 6); minor phases include hornblende, apatite, zircon, ilmenite, magnetite, and myrmekite. Lincoln Granite is far less abundant than Sherman Granite. Geochemically, Lincoln Granite overlaps with the most evolved portions of the Sherman Granite, with relatively high silica content and low iron enrichment. The Lincoln Granite is classified as a ferroan alkali-calcic peraluminous granitoid (Frost and Frost, 1997). Contacts with the Sherman Granite are sharp. Contacts with the porphyritic granite are mingled to sharp. Some samples include isolated alkali feldspar megacrysts that comprise less than 1 percent of the rock (Frost and others, 1999).

One sample of the Lincoln Granite (20130703JC-H) within the map area was analyzed for major element, minor element, and REE compositions. This sample generally falls within the low-silica end of the composition range of the Lincoln Granite in the Sherman Mountains area to the north (Frost and others, 1999); however, this sample is more potassic than the Lincoln Granite in the Sherman Mountains (Fig. 2). The REE content of sample 20130703JC-H is similar to the Lincoln Granite analyzed by Frost and others (1999), though sample 20130703JC-H is slightly more enriched in the heavy REE (Fig. 3).

The Lincoln Granite is dated at $1,430 \pm 2.6$ Ma by U-Pb dating (Frost and others, 1999). It was named after the Lincoln Monument that is present on the summit of the old Lincoln Highway and Interstate 80 (Edwards, 1993).

Middle Proterozoic Monzodiorite (Ym) and Mafic Dikes (Ymd)

Fine-grained, brown to purple-black, highly fractured and weathered monzodiorite (Fig. 7) in the map area crops out as elongate pods that cut the Sherman Granite and is spatially associated with the porphyritic granite. Monzodioritic and diabasic dikes (Fig. 8) are common throughout the map area, and are generally associated with 340° – 350° trending fractures and faults. Major phases within the monzodiorite are plagioclase, biotite, quartz, and orthoclase (Fig. 9); minor phases include apatite, epidote, ilmenite, magnetite, and titanite. Sparse plagioclase megacrysts are present at some locations, as are alkali feldspars megacrysts that can display thin rims of plagioclase. The diabasic dikes exhibit tabular plagioclase phenocrysts up to ~1.5 mm (0.059 in) in length hosted in an aphanitic matrix (Fig. 10). However, samples of the monzodiorite (20130620JC-A) and a diabasic dike (20130703JC-C) are nearly geochemically identical. Plagioclase xenocrysts associated with small round quartz grains and hornblende are seen in random locations in the field (Frost and others, 1999). Two varieties of monzodiorite bodies have been recognized within the Sherman batholith that include an Fe-rich commingled body and an Mg-rich body that had less interaction with local

country rock (Edwards, 1993). Mg-rich monzodiorite bodies are apparently the most abundant variety within the map area, and represent the primitive end of the geochemical array defined by the rocks of the Sherman batholith (Fig. 2). The mafic rocks from the map area have similar REE concentrations (Fig. 3) to those in the Sherman Mountains area (Frost and others, 1999).

The monzodiorite bodies have not been dated using modern isotope methods. However, monzodiorite bodies within the mapping area cross-cut Sherman Granite, Lincoln Granite enclaves and dikes, and porphyritic granite, but are also cut by Lincoln Granite dikes and exhibit gradational contacts and comingling with the porphyritic granite. These field relationships indicate a syn-Sherman batholith emplacement history.

Middle Proterozoic Porphyritic Granite (Yp)

The porphyritic granite (Fig. 11) is medium-grained, orange-gray to brown biotite hornblende granite with 1 to 4 cm (0.4 to 1.6 in), orange-pink and pink-gray perthitic microcline, and some plagioclase phenocrysts that show rapakivi-texture of plagioclase and quartz rims. Major phases include perthitic microcline, plagioclase, quartz, biotite, hornblende; minor phases include ilmenite, apatite, zircon, titanite, and pigeonite. The porphyritic granite crops out as large irregular bodies and as thin dikes that cut the Sherman Granite. Some outcrops of porphyritic granite show orientation of phenocrysts in a single stress direction related to local emplacement deformation. The porphyritic granite (named by Edwards, 1993) is considered a composition intermediate between the Sherman and Lincoln Granites (Frost and others, 1999); a sample of porphyritic granite (20130613BG-1) from the map area generally plots within the primitive end of compositional ranges reported by Frost and others (1999) in the Sherman Mountains area (Fig. 2). The REE composition of sample 20130613BG-1 (Fig. 3) is similar to that of the porphyritic granite analyzed by Frost and others (1999).

No absolute ages of the porphyritic granite are available. Frost and others (1999) estimated the porphyritic granite to be between 1,430 and 1,433 Ma based on the modal composition association between the Lincoln and Sherman Granites.

Middle Proterozoic Sherman Granite (Ys)

The main-phase of the Sherman Granite (Fig. 12) is a very coarse-grained, pink to reddish-orange, biotite hornblende granite, quartz monzonite, and monzonite that crops out in rounded to craggy mounds and more commonly a thick weathered gus. The dominant mineral phases of the Sherman Granite include microcline, perthite, plagioclase, quartz, biotite, hornblende, and ilmenite (Fig. 13); minor phases include zircon and apatite, and in some locations augite, pigeonite, and fayalite. The Sherman Granite has a subporphyritic granular texture, exhibiting megacrystic microcline rimmed in plagioclase resulting in rapakivi texture in some locations. Feldspar megacrysts are typically tabular, and range from 1 to 4 cm (0.4 to 1.6 in) in length. Minor concentric zoning is present in plagioclase.

Sherman Granite is the most aurally extensive exposed unit of the Sherman batholith. Within the map area, the main phase of the Sherman Granite ranges in composition from relatively primitive, with low silica and high iron concentrations (compared to the Lincoln Granite) to nearly identical to the Lincoln Granite (Fig. 2). The Sherman Granite is classified as a ferroan alkali-calcic metaluminous granitoid (Frost and Frost, 1997). Minor enclaves of Lincoln Granite, porphyritic granite, and monzodiorite are locally present within the main phase of the Sherman Granite (Fig. 14). Contacts with both the Lincoln Granite and the porphyritic granite tend to be sharp. Two samples (20121107JC-A and 20130626JC-A) of fresh, unaltered Sherman Granite were analyzed for major element, minor element, and REE concentrations. These two samples, in general, span the compositional ranges of the Sherman Granite in the Sherman Mountains area (Fig. 2; Frost and others, 1999). Compared to the Sherman Granite in the Sherman Mountains with similar silica content, the sample from the map area with the lower silica content (20121107JC-A) is enriched in Na_2O , K_2O , and Al_2O_3 , and depleted in CaO and TiO_2 (Fig. 2). The two samples from the Dale Creek area generally match the REE compositions of the Sherman Granite in the Sherman Mountains area (Frost and others, 1999), although sample 20121107JC-A does not exhibit a strong Eu-anomaly (Fig. 3).

Near its contact with the porphyritic granite and the biotite gneiss, epidote, hematite, and calcium-enrichment are present in the Sherman Granite. Three samples (20130628JC-B, 20130628JC-C, and 20121129BG-2) of Sherman Granite with moderate epidote and/or hematite alteration were analyzed for major element, minor element, and REE compositions. Sample 20130628JC-B plots well outside of the compositional range of the Sherman Granite in the Sherman Mountains area, due to low silica content, the other two samples generally plot near the edge of the compositional ranges in the Sherman Mountains area (Fig. 2). However, the two samples with typical silica content (20130628JC-C and 20121129BG-2) exhibit relatively high sodium concentrations, and one of these, along with the low-silica sample, exhibit elevated calcium concentrations. The epidote- and iron-alteration is likely a product of alteration associated with fluids driven off from the porphyritic granite and biotite gneiss. It is possible that the high-sodium samples represent enclaves of sodic rocks within the Sherman Granite. However, the samples with high sodium content have much higher Na_2O concentrations than the sodic rocks in the Sherman Mountains area, and plot within the normal range of Sherman Granite for normalized REE concentrations, and an order of magnitude higher than the sodic rocks reported by Frost and others (1999). Similar to sample 20121107JC-A, 20121129BG-2 does not exhibit a strong Eu-anomaly (Fig. 3).

Near its contact with Early Proterozoic biotite gneiss, the main phase of the Sherman Granite is medium- to coarse-grained, but the overall texture is similar to that of the main phase elsewhere in the mapping area. In the southeastern corner of the map area, the Sherman Granite hosts a large gabbro enclave consisting of plagioclase and pyroxenes that have been partially altered to hornblende. Geochemical analyses (Sample 20130703JC-G) show that this gabbro is distinctly more primitive (lower silica content and higher MgO and CaO concentrations) than the other mafic rocks in the map area (Fig. 2). This gabbro was not observed elsewhere within the map area.

The Sherman Granite has been dated at $1,433 \pm 1.5$ Ma by U-Pb dating (Frost and others, 1999).

Middle Proterozoic Sherman Granite Inner Cap Rock Phase (Ysi)

The inner cap rock phase of the Sherman Granite (Fig. 15) consists of coarse-grained, pinkish-gray, porphyritic, biotite granite to quartz monzonite. In places, the inner cap rock phase exhibits a foliation defined by oriented tabular microcline phenocrysts, biotite-rich streaks, and oriented tabular inclusions (Eggler and Braddock, 1988). Major phases of the inner cap rock phase include microcline, perthite, plagioclase, quartz, biotite, and magnetite (Fig. 16); minor phases include apatite, zircon, allanite, titanite, and fluorite (Eggler, 1968). Contacts with the outer cap rock phase are typically gradational over distances up to several hundred meters (Eggler and Braddock, 1988), but locally can be sharp. Contacts with the Sherman Granite are sharp. One sample of the inner cap rock phase (20130703JC-A) was analyzed geochemically. This sample falls outside of the compositional ranges of the Sherman Granite in the Sherman Mountains area (Frost and others, 1999) due to relatively high silica content (Fig. 2). Sample 20130703JC-A is depleted in all but the lightest REE, compared to the Sherman Granite samples (Fig. 3).

Middle Proterozoic Sherman Granite Outer Cap Rock Phase (Yso)

The outer cap rock phase of the Sherman Granite (Fig. 17) is nearly compositionally identical to the inner cap rock phase. However, the outer cap rock phase is finer-grained with more abundant biotite streaks and a higher average color index (Eggler, 1968). Phenocrysts are generally smaller than in the inner cap rock phase, but not always present. When present, the phenocrysts can be oriented (Eggler and Braddock, 1988). No geochemical analyses were performed on the outer cap rock phase.

Early Proterozoic Metamorphic Rocks

Early Proterozoic Biotite Gneiss (Xbg)

Present in the southeastern corner of the map area is gray, pink, or red, medium-grained biotite gneiss, composed mostly of quartz, plagioclase, and microcline. Biotite constitutes 10 to 20 percent of the rock. Garnet is present but rare. Secondary opaque oxides are present in some samples. Biotite occurs as anastomosing seams and elongate, flattened discoid groups that are uniformly distributed in the rock. Contacts with adjacent rocks are generally concordant to foliation, but are discordant in places (Eggler and Braddock, 1988). Major phases include quartz, plagioclase, microcline, and biotite; minor phases include garnet and opaque oxides. Sample 12DC-1 was dated at $1,771 \pm 6$ Ma by U-Pb dating (see Appendix for complete analyses). This sample was also analyzed for major element, minor element, and REE compositions.

REFERENCES

- Aleinkoff, J.N., 1983, U-Th-Pb systematics of zircon inclusions in rock-forming minerals—A study of armoring against isotopic loss using the Sherman granite of Colorado–Wyoming, USA: *Contributions to Mineralogy and Petrology*, v. 82, p. 259–269.
- DePaolo, D.J., 1981, Neodymium isotopes in the Colorado Front Range and crust–mantle evolution in the Proterozoic: *Nature*, v. 291, p. 193–196.
- Edwards, B.R., 1993, A field, geochemical, and isotopic investigation of the igneous rocks in the Pole Mountain area of the Sherman batholith, southern Laramie Mountains, Wyoming, U.S.A.: M.S. thesis, University of Wyoming, Laramie, 164 p., scale 1:24,000.
- Edwards, B.R., and Frost, C.D., 2000, An overview of the petrology and geochemistry of the Sherman batholith, southeastern Wyoming—Identifying multiple sources of Mesoproterozoic magmatism: *Rocky Mountain Geology*, v. 35, no. 1, p. 113–137.
- Eggler, D.H., 1968, Virginia Dale Precambrian ring-dike complex, Colorado-Wyoming: *Geological Society of America Bulletin*, v. 79, p. 1545–1564.
- Eggler, D.H., and Braddock, W.A., 1988, Geologic map of the Cherokee Park Quadrangle, Larimer County, Colorado and Albany County, Wyoming: U.S. Geological Survey Geologic Quadrangle Map GQ-1615, scale 1:24,000.
- Frost, C.D., Chamberlain, K.R., Frost, B.R., and Scoates, J.S., 2000, The 1.76 Ga Horse Creek anorthosite complex, Wyoming—A massif anorthosite emplaced late in the Medicine Bow Orogeny: *Rocky Mountain Geology*, v. 35, no. 1, p. 71–90.
- Frost, C.D., and Frost, B.R., 1997, Reduced rapakivi-type granites—The tholeiite connection: *Geology*, v. 25, no. 7, p. 647–650.
- Frost, C.D., Frost, B.R., Chamberlain, K.R., and Edwards, B.R., 1999, Petrogenesis of the 1.43 Ga Sherman batholith, SE Wyoming, USA—A reduced, rapakivi-type anorogenic granite: *Journal of Petrology*, v. 40, no. 12, p. 1771–1802.
- Frost, C.D., Meier, M., and Oberli, F., 1990, Single zircon U-Pb age determination of the Red Mountain Pluton, Laramie Anorthosite Complex, Wyoming: *American Mineralogist*, v. 75, p. 21–26.
- Harrison, J.E., 1951, Relationship between structure and mineralogy of the Sherman granite, southern part of the Laramie Range, Wyoming–Colorado border: Urbana, University of Illinois, Ph.D. thesis, 79 p.
- Hausel, W.D., McCallum, M.E., and Woodzick, T.L., 1979, Exploration for diamond-bearing kimberlite in Colorado and Wyoming: an evaluation of exploration techniques: Wyoming State Geological Survey Report of Investigations 19, 29 p.
- Houston, R.S., and Marlatt, G., 1997, Proterozoic geology of the Granite Village area, Albany and Laramie Counties, Wyoming, compared with that of the Sierra Madre and Medicine Bow

- Mountains of southeastern Wyoming: U.S. Geological Survey Bulletin 2159, 25 p., 1 pl., scale 1:24,000.
- Jones, D.S., Snoke, A.W., Premo, W.R., and Chamberlain, K.R., 2010, New models for Paleoproterozoic orogenesis in the Cheyenne belt region—Evidence from the geology and U-Pb geochronology of the Big Creek Gneiss, southeastern Wyoming: *Geological Society of America Bulletin*, v. 122; no. 11–12; p. 1877–1898. doi:10.1130/B30164.1
- Krogh, T.E., 1973, A low-contamination method for hydrothermal decomposition of zircon and extraction of U and Pb for isotopic age determinations: *Geochimica et Cosmochimica Acta*, v. 37, p. 485–494.
- Ludwig, K.R., 1988, PBDAT for MS-DOS, a computer program for IBM-PC compatibles for processing raw Pb-U-Th isotope data, version 1.24: U.S. Geological Survey Open-File Report 88-542, 32 p.
- Ludwig, K.R., 1991, ISOPLOT for MS-DOS, a plotting and regression program for radiogenic-isotope data, for IBM-PC compatible computers, version 2.75: U.S. Geological Survey Open-File Report 91-445, 45 p.
- Masuda, A., Nakamura, N. and Tanaka, T., 1973, Fine structures of mutually normalized rare-earth patterns of chondrites: *Geochimica et Cosmochimica Acta*, v. 37, p. 239–248.
- Mattinson, J.M., 2005, Zircon U-Pb chemical abrasion (“CA-TIMS”) method—Combined annealing and multi-step partial dissolution analysis for improved precision and accuracy of zircon ages: *Chemical Geology*, v. 220, p. 47–66.
- McCallum, M.E., Eggler, D.H., and Burns, L.K., 1975, Kimberlitic diatremes in northern Colorado and southern Wyoming: *Physics and Chemistry of the Earth*, v. 9, p. 149–161.
- Nicoll, G.A., 1963, Geology of the Hutton Lake anticline area, Albany County, Wyoming: Laramie, University of Wyoming, M.S. thesis, 80 p., 1 plate, scale 1:35,200.
- Parrish, R.R., Roddick, J.C., Loveridge, W.D., and Sullivan, R.D., 1987, Uranium-lead analytical techniques at the geochronology laboratory, Geological Survey of Canada, *in* Radiogenic age and isotopic studies, Report 1: Geological Survey of Canada Paper 87-2, p. 3–7.
- Reed, J.C., Jr., Bickford, M.E., Premo, W.R., Aleinkoff, J.N., and Pallister, J.S., 1987, Evolution of the Early Proterozoic Colorado Province: Constraints from U-Pb geochronology: *Geology*, v. 15, p. 861–865.
- Steiger, R.H., and Jäger, E., 1977, Subcommittee on geochronology—Convention on the use of decay constants in geo- and cosmochronology: *Earth and Planetary Science Letters*, v. 36, p. 359–362.
- Sutherland, W.M., Gregory, R.W., Carnes, J.D., and Worman, B.W., 2013, Rare earth elements in Wyoming: Wyoming State Geological Survey Report of Investigations 65, 82 p.
- Vasek, R.W., and Kolker, A., 1999, Virginia Dale intrusion, Colorado and Wyoming—Magma-mixing and hybridization in a Proterozoic composite intrusion: *Rocky Mountain Geology*, v. 34,

no. 2, p. 195–222.

Ver Ploeg, A.J., 1999, Reconnaissance/photogeologic map of the Dale Creek Quadrangle, Albany County, Wyoming: Wyoming State Geological Survey files (unpublished), scale 1:24,000.

Ver Ploeg, A.J., Bagdonas, D., and McLaughlin, J.F., 2011, Preliminary geologic map of the Best Ranch quadrangle, Albany County, Wyoming: Wyoming State Geological Survey Open File Report 11-7, scale 1:24,000.

Ver Ploeg, A.J., and Boyd, C.S., 2007, Geologic map of the Laramie 30' x 60' quadrangle, Albany and Laramie counties, southwestern Wyoming: Wyoming State Geological Survey Map Series 77, scale 1:100,000.

FIGURES AND TABLES



Figure 1. Field photograph showing the Sherman Granite in contact with the underlying Fountain Formation.

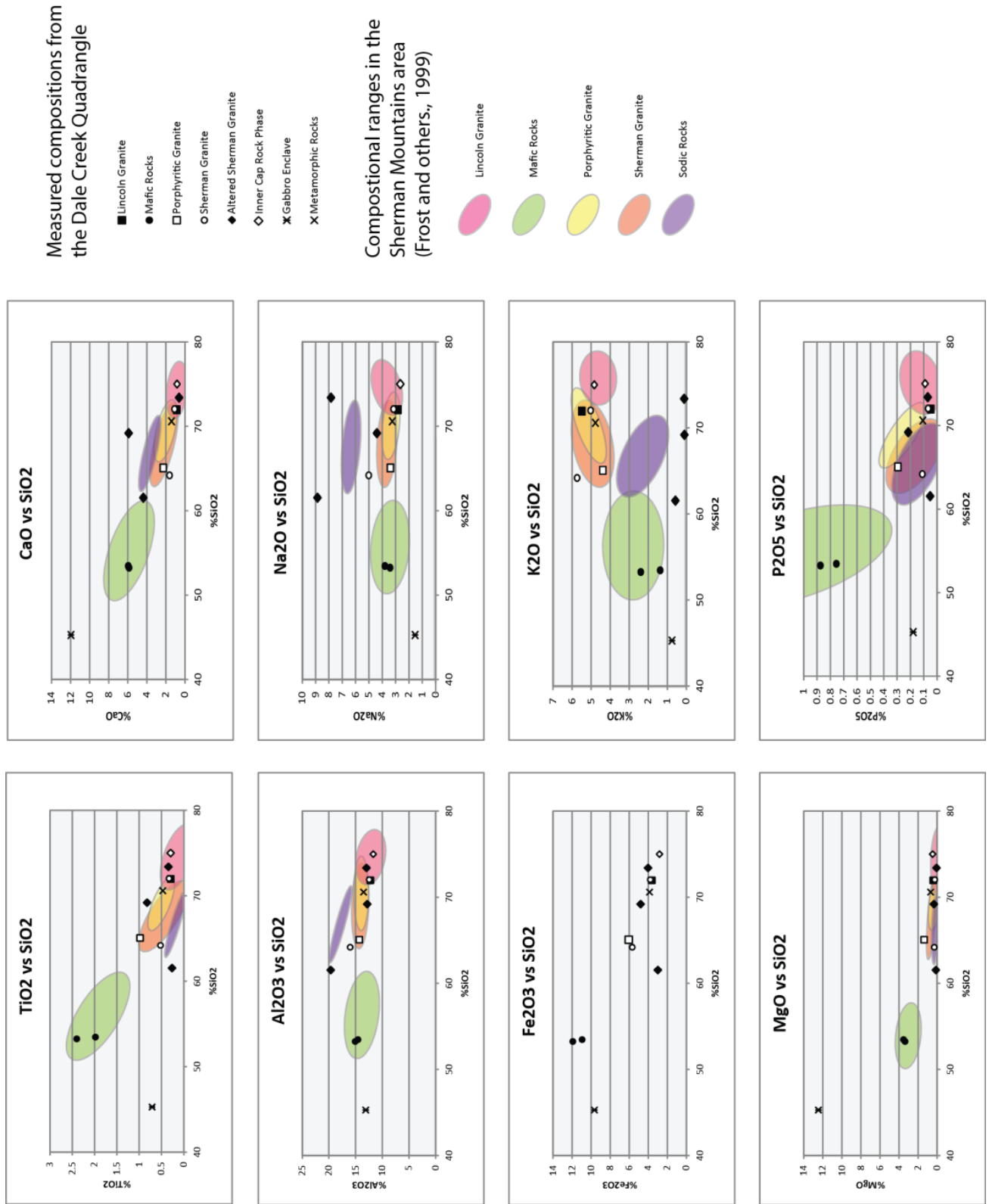


Figure 2. Major element compositions, as oxides, of samples from the map area compared to the compositional ranges reported by Frost and others (1999).

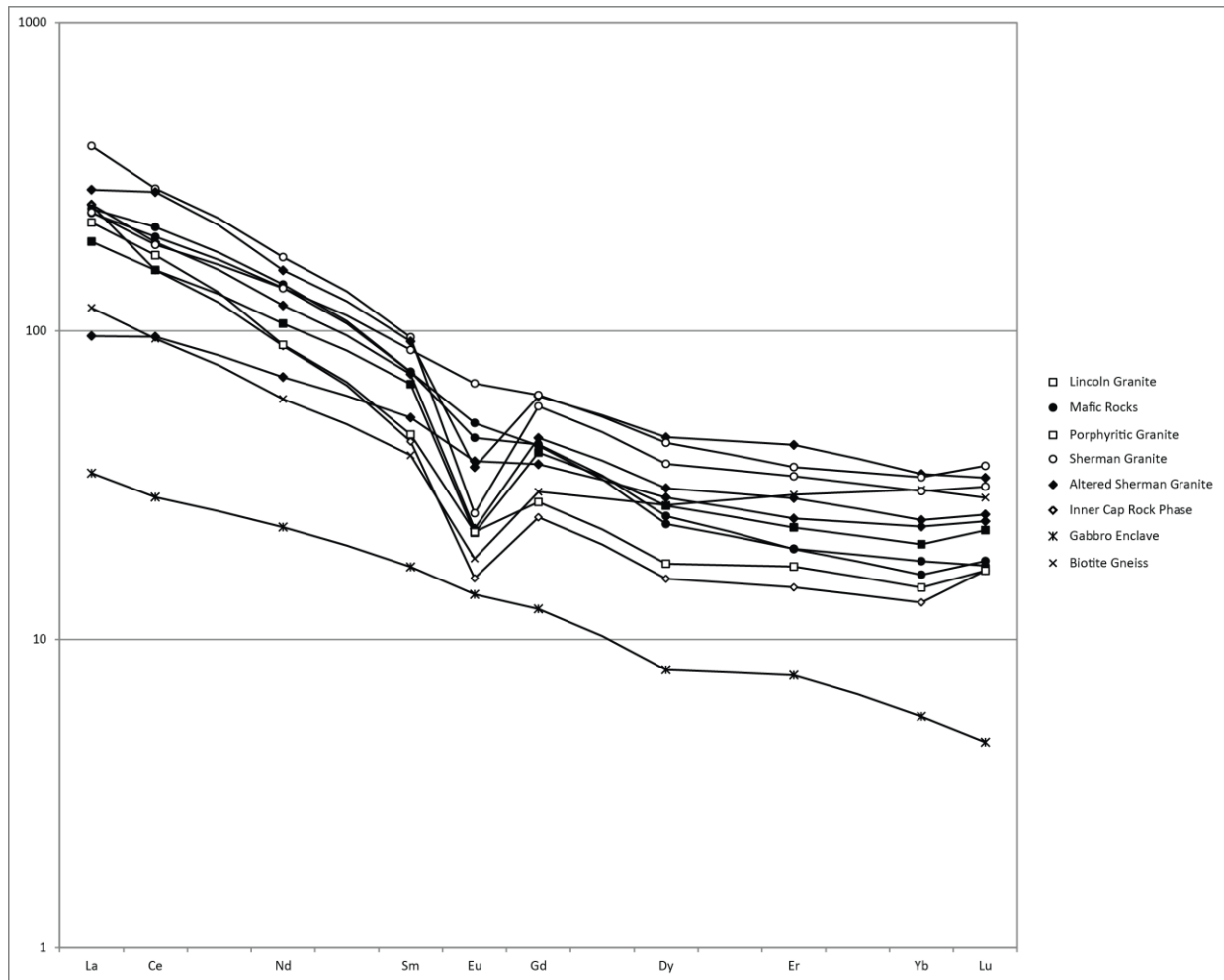


Figure 3. Rare earth element concentrations of samples from the Dale Creek quadrangle, normalized after Masuda and others (1973).



Figure 4. Field photo of the Lincoln Granite.



Figure 5. Field photo of a dike of Lincoln Granite cutting across low-lying, grus-covered Sherman Granite.

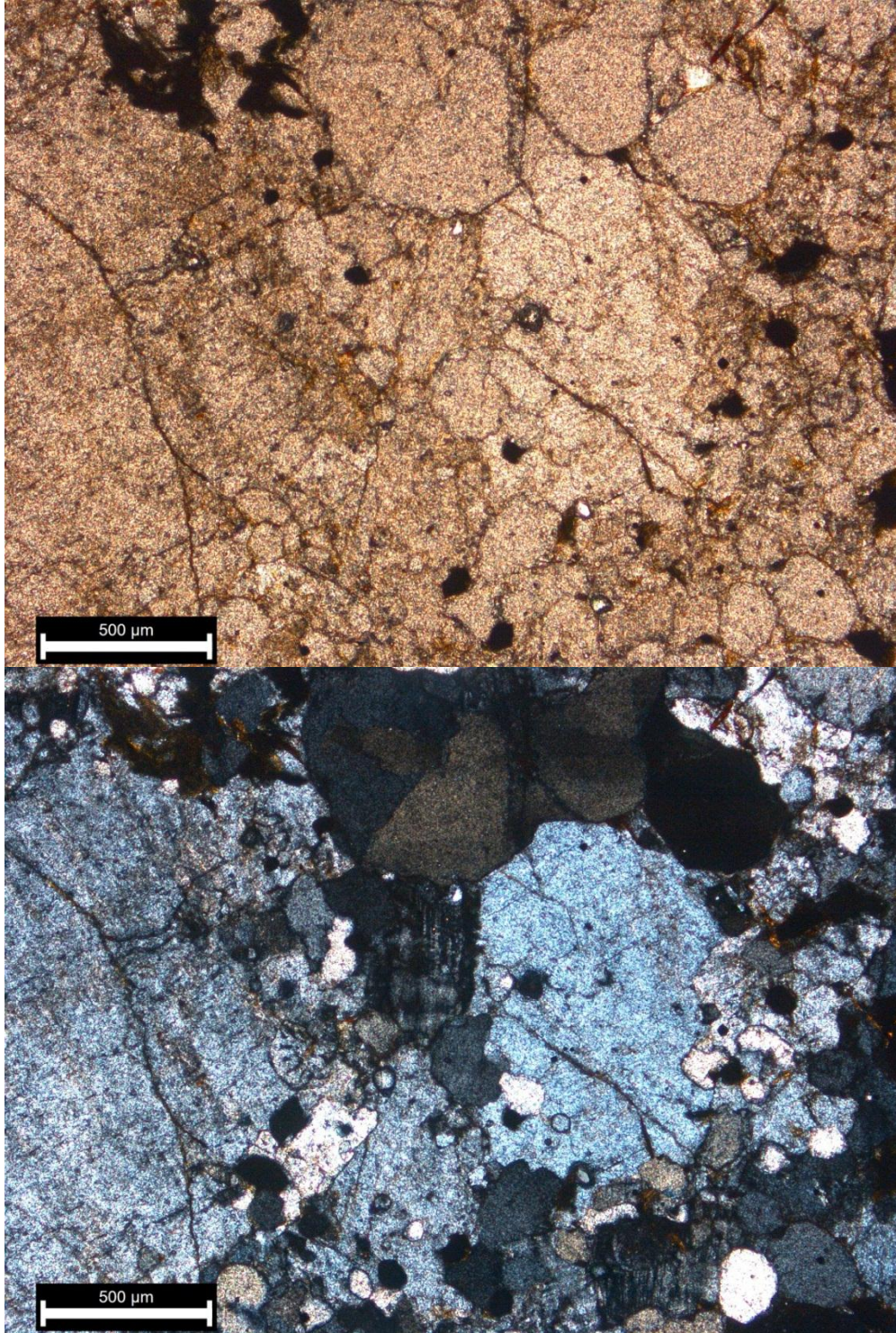


Figure 6. Photomicrographs of the Lincoln Granite in plane polarized light (top) and cross polarized light (bottom). Phases within the field of view include perthite, quartz, microcline, biotite, plagioclase, and ilmenite and/or magnetite.



Figure 7. Field photo of monzodiorite with minor alkali feldspar phenocrysts.



Figure 8. Field photo showing a diabasic dike cutting the Sherman Granite. Dike is represented by sub-vertical grassy band within the pink Sherman Granite in the middle of the photograph.

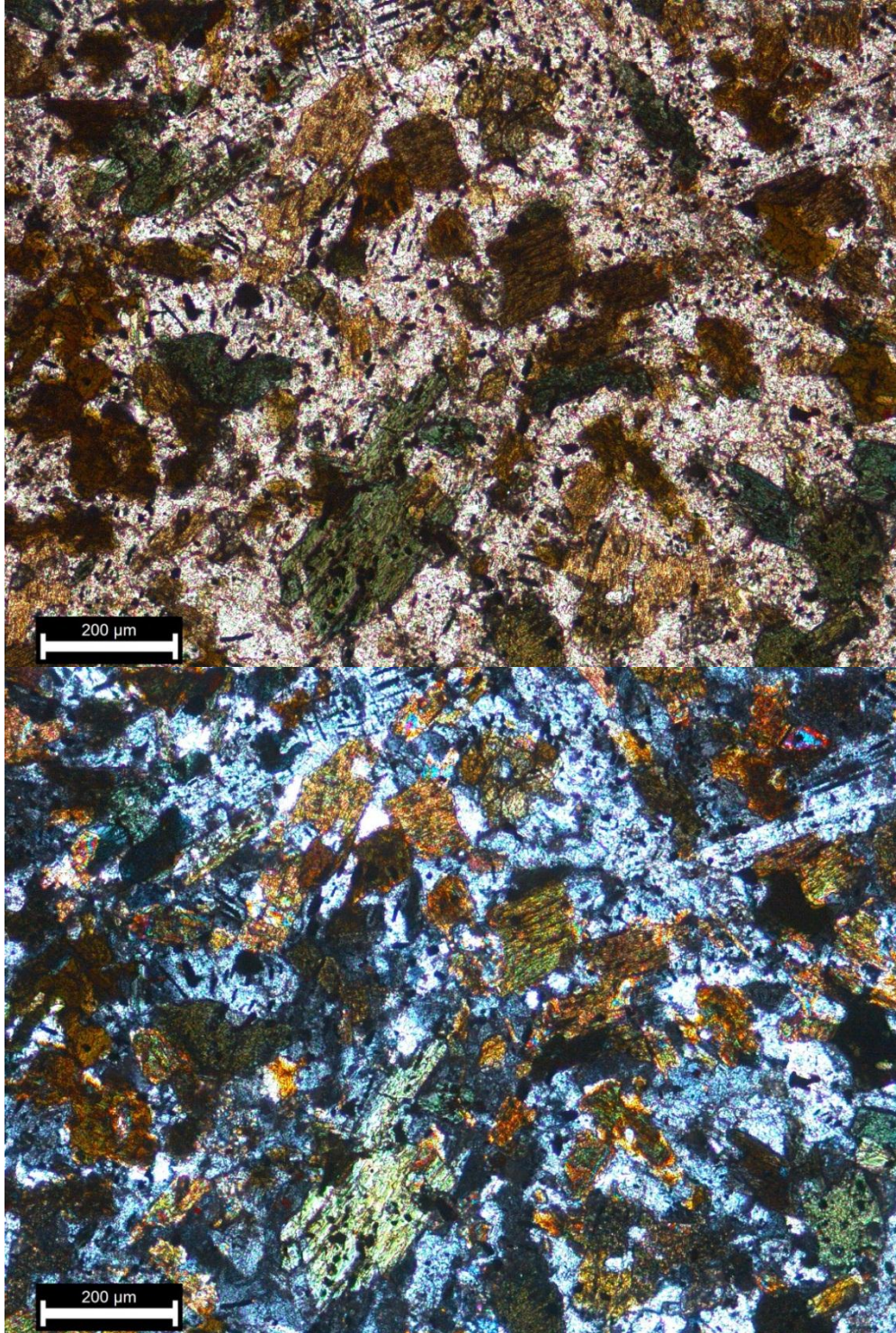


Figure 9. Photomicrographs of monzodiorite in plane polarized light (top), and cross polarized light (bottom). Phases present in the field of view include plagioclase, biotite, quartz, alkali feldspar, hornblende, and ilmenite and/or magnetite.

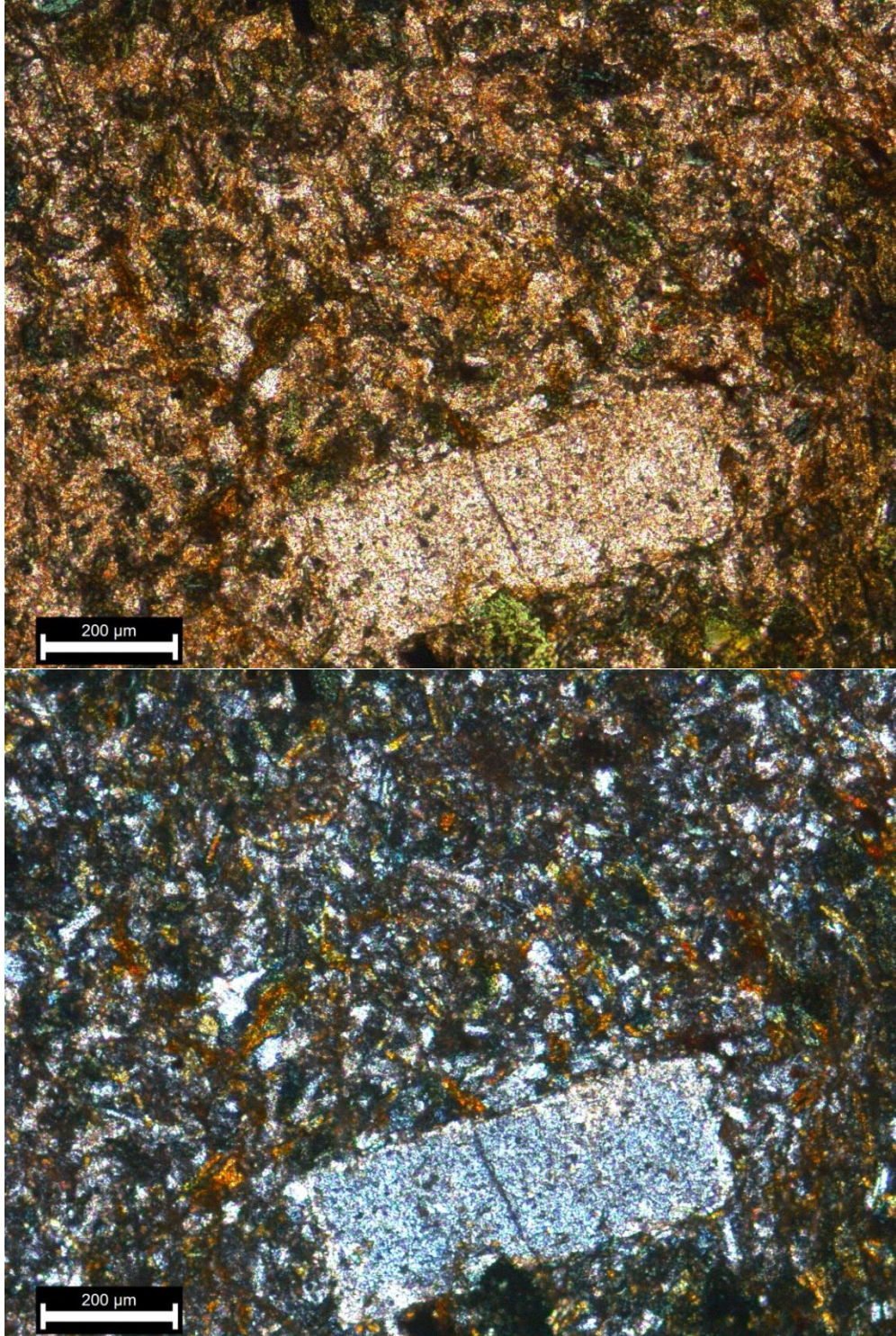


Figure 10. Photomicrographs of diabasic dike in plane polarized light (top), and cross polarized light (bottom). Phases present in the field of view include plagioclase, biotite, quartz, alkali feldspar, and ilmenite and/or magnetite. The large crystal near the bottom is plagioclase with sericite alteration.



Figure 11. Field photo of porphyritic granite.



Figure 12. Field photo of the main phase of Sherman Granite

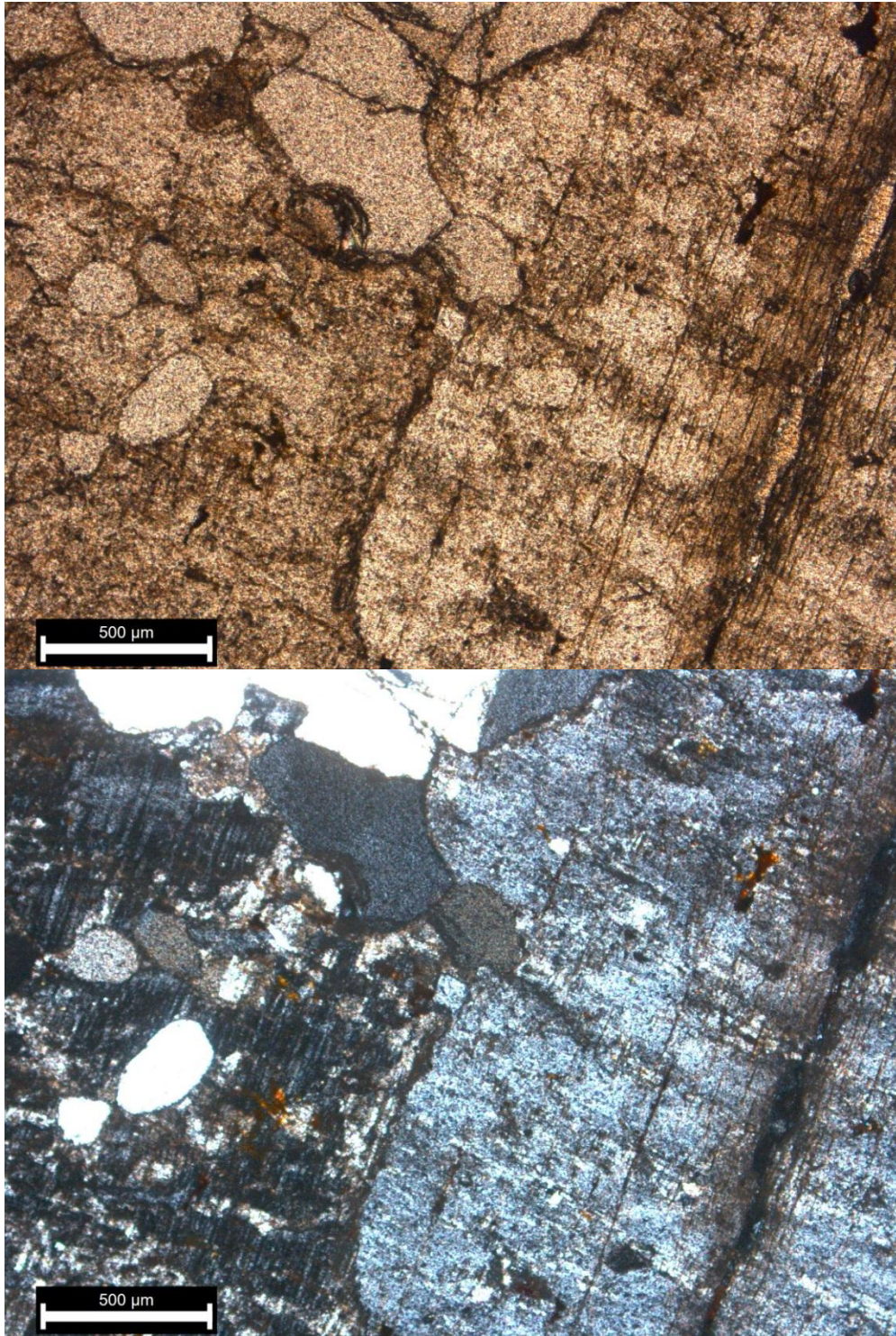


Figure 13. Photomicrographs of Sherman Granite in plane polarized light (top), and cross polarized light (bottom). Phases present in the field of view include perthite, quartz, microcline, and plagioclase.



Figure 14. Field photograph showing an enclave of Lincoln Granite hosted within the main phase of Sherman Granite.



Figure 15. Field photograph of the inner cap rock phase of Sherman Granite.

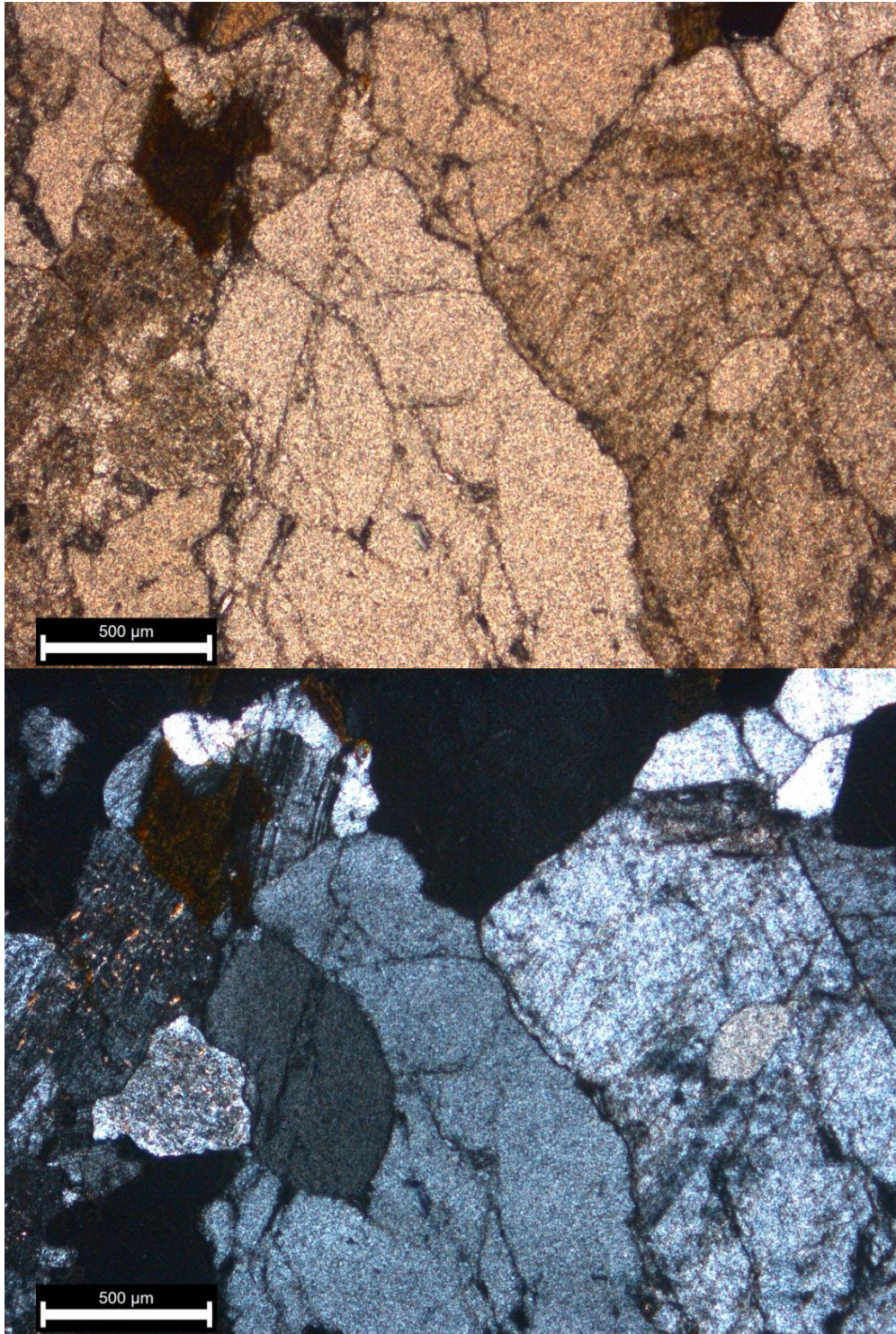


Figure 16. Photomicrographs of the inner cap rock phase of Sherman Granite in plane polarized light (top), and cross polarized light (bottom). Phases present in the field of view include perthite, quartz, plagioclase, and biotite.



Figure 17. Field photo of the outer cap rock phase of Sherman Granite.

Table 1. Major element analyses of samples from the Dale Creek quadrangle. Sample locations shown on map.

Sample	20130703JC-H	20130620JC-A	20130703JC-C	20130613BG-1	20121107JC-A*	20130626JC-A	20121129BG-2*	20130628JC-B	20130628JC-C	20130703JC-A	20130703JC-G	12DC-1
Unit	Lincoln Granite	Monzodiorite	Diabasic Dike	Porphyritic Granite	Sherman Granite	Sherman Granite	Altered Sherman Granite	Altered Sherman Granite	Altered Sherman Granite	Inner Cap Rock Phase	Gabbro Enclave	Biotite Gneiss
SiO ₂	71.97	53.26	53.47	65.07	64.2	72.04	73.4	61.55	69.2	75.01	45.29	70.6
Al ₂ O ₃	12.22	15.06	14.55	14.28	16	12.42	12.95	19.65	12.8	11.67	13.08	13.48
Fe ₂ O ₃	3.62	11.91	10.93	6.04	5.67	3.78	4.01	2.99	4.79	2.82	9.64	3.85
CaO	0.85	5.85	5.93	2.26	1.6	1.08	0.6	4.35	5.89	0.81	11.95	1.39
MgO	0.4	3.35	3.51	1.35	0.29	0.24	0.05	0.12	0.33	0.46	12.45	0.67
Na ₂ O	2.82	3.41	3.8	3.38	5.01	3.15	7.84	8.85	4.4	2.64	1.53	3.24
K ₂ O	5.48	2.39	1.37	4.38	5.73	5.02	0.11	0.57	0.1	4.83	0.75	4.77
Cr ₂ O ₃	0.01	0.01	0.02	0.01	<0.01	0.01	<0.01	0.01	0.01	0.01	0.08	0.01
TiO ₂	0.29	2.4	1.98	0.98	0.52	0.33	0.34	0.26	0.82	0.29	0.71	0.47
MnO	0.05	0.14	0.17	0.08	0.09	0.07	0.01	0.06	0.07	0.05	0.16	0.02
P ₂ O ₅	0.047	0.874	0.755	0.293	0.11	0.067	0.07	0.052	0.216	0.089	0.179	0.106
SiO	0.01	0.08	0.05	0.04	0.02	0.02	0.01	0.08	0.08	0.02	0.04	0.02
BaO	0.05	0.14	0.13	0.15	0.23	0.08	<0.01	0.04	0.02	0.09	0.05	0.11
LOI	0.34	0.8	2.37	0.68	0.98	0.36	0.56	0.62	0.87	0.44	2.41	0.31
Total	98.17	99.67	99.04	98.99	100.45	98.67	99.95	99.19	99.58	99.23	98.32	99.04
Na₂O + K₂O	8.30	5.80	5.17	7.76	10.74	8.17	7.95	9.42	4.50	7.47	2.28	8.01
A/CNK	1.01	0.80	0.79	0.99	0.92	0.99	0.92	0.85	0.71	1.06	0.52	1.04
Fe₂O₃/(Fe₂O₃ + MgO)	0.90	0.78	0.76	0.82	0.95	0.94	0.99	0.96	0.94	0.86	0.44	0.85

*Samples from Sutherland and others, 2013

Table 2. Minor element analyses of samples from the Dale Creek quadrangle. Sample locations shown on map.

Sample	20130703JC-H	20130620JC-A	20130703JC-C	20130619BG-1	20121107JC-A*	20130626JC-A	20121129BG-2*	20130628JC-B	20130628JC-C	20130703JC-A	20130703JC-G	12DC01
Unit	Lincoln Granite	Monzodiorite	Diabasic Dike	Porphyritic Granite	Sherman Granite	Sherman Granite	Altered Sherman Granite	Altered Sherman Granite	Altered Sherman Granite	Inner Cap Rock Phase	Gabbro Enclave	Biotite Gneiss
Ba	438	1230	1130	1325	2100	714	19.9	215	32.4	713	318	914
Ce	128	164	176.5	143	154.5	235	77.8	157.5	229	128	23.5	76.7
Cr	20	20	70	10	10	10	10	10	10	10	510	20
Cs	0.63	1.12	0.69	2.43	0.9	0.79	0.07	0.38	0.49	2.08	1.63	2.13
Dy	8.81	7.69	8.16	5.72	14.1	12.05	9.37	10.05	14.7	5.11	2.59	8.86
Er	4.91	4.19	4.18	3.67	7.71	7.2	5.25	6.11	9.1	3.14	1.63	6.27
Eu	1.6	3.63	3.25	1.61	4.88	1.85	2.73	1.65	2.61	1.14	1.01	1.32
Ga	24.8	26.7	25.6	23.6	23.8	25.5	22.1	39.9	27.1	20	13.7	20.8
Gd	10.45	11	11.1	7.22	16.05	14.75	9.57	11.65	15.9	6.44	3.25	7.79
Hf	13.9	9.9	10.4	8.6	25.2	14.3	15.2	11.3	14.8	7.2	1.3	9.8
Ho	1.76	1.58	1.66	1.17	2.82	2.58	1.88	2.1	3.1	1.13	0.5	2.07
La	61.3	75.9	78.4	70.7	76.4	125	30.3	80.9	90.3	80.3	10.9	37.4
Lu	0.73	0.56	0.58	0.54	1.18	1.01	0.78	0.82	1.08	0.54	0.15	0.93
Nb	10.9	27.4	24.3	17.7	42.5	27.3	34.1	22	36.6	16.9	3.2	19.1
Nd	63	82.3	84.4	53.8	82.1	103.5	42.3	72.2	93.8	53.3	13.8	35.9
Pr	15.7	19.4	20.6	14.9	20.5	26.1	10.05	18.9	23	15.3	3.05	9.15
Rb	99.2	64.1	41.9	152	122.5	129	2.3	11.3	2.6	216	28.5	161.5
Sm	12.9	14.1	14.15	8.86	16.65	18.3	10.05	13.9	17.75	8.41	3.3	7.59
Sn	1	3	2	2	2	2	1	1	2	2	1	3
Sr	48.9	542	388	262	141	75	65.1	540	569	108	302	91.4
Ta	0.5	1.2	1.2	0.8	2.4	1.4	1.6	1.2	1.9	1	0.2	1.1
Tb	1.83	1.73	1.82	1.19	2.46	2.45	1.57	2.04	2.79	1.04	0.5	1.59
Th	7.46	7.58	12.85	19.95	14.2	18.4	10.75	13.25	17.05	39.7	1.22	16.75
Tl	0.9	<0.5	<0.5	0.8	0.6	0.8	<0.5	<0.5	<0.5	1.1	<0.5	0.5
Tm	0.7	0.58	0.58	0.52	1.11	0.98	0.75	0.78	1.15	0.55	0.19	0.95
U	2.39	2.62	3.98	7.87	8.72	4.7	2.32	4.01	3.93	8.74	0.54	3.35
V	6	176	164	64	7	7	7	10	24	18	207	35
W	2	2	2	3	1	5	1	2	2	2	3	3
Y	37.6	40.1	43.3	31.1	65.7	64.8	48.7	50.4	82.4	28.7	15.7	52.4
Yb	4.23	3.73	3.37	3.06	6.98	6.29	4.83	5.07	7.15	2.74	1.17	6.36
Zr	546	432	431	329	997	515	636	392	555	245	52	331
Rb/Ba	0.23	0.05	0.04	0.11	0.06	0.18	0.12	0.05	0.08	0.30	0.09	0.18
Rb/Sr	2.03	0.12	0.11	0.58	0.87	1.72	0.04	0.02	0.00	2.00	0.09	1.77
Ce/Yb	30.26	43.97	52.37	46.73	22.13	37.36	16.11	31.07	32.03	46.72	20.09	12.06

* Samples from Sutherland and others, 2013

APPENDIX

The information presented here includes the relevant data used to calculate the radiometric date of $1,771 \pm 6$ Ma for sample 12DC-1 (see map for sample location) of the Early Proterozoic biotite gneiss. Data and description are by Dr. Kevin Chamberlain, Research Professor, University of Wyoming.

Zircons separated from the biotite gneiss were pretreated by chemical abrasion (Mattinson 2005) to minimize the effects of Pb loss on the data. The chemical abrasion method involves annealing the zircons at 850 °C for 48 hours prior to a 2-step dissolution. The first, low-temperature dissolution step removes uranium rich, metamict zones that are most susceptible to the effects of Pb loss. For sample 12DC-1, the zircons appear to represent a single morphological population. Many of the grains are cracked and Fe-stained, and the first step of dissolution mined out significant portions of the grains (Figure 18). The U-Pb data come from final dissolution of individual, skeletal shards of the remnant, low-uranium domains. Analytical procedures are detailed in Table 3. Data from three individual grains are concordant or nearly concordant and overlap within error (Figure 19) with a weighted mean date of $1,771 \pm 6$ Ma (Figure 20, Table 3). The zircons are interpreted to represent a single period of zircon growth due to the consistency of dates and the similarity in morphologies. The zircon morphologies are typical of magmatic growth, but a metamorphic origin is also possible. The low $^{208}\text{Pb}/^{206}\text{Pb}$ from these analyses (0.08 to 0.05, Table 3) are consistent with metamorphic zircon growth, but are not diagnostic alone. Magmatic systems with low Th/U will also produce zircons with low $^{208}\text{Pb}/^{206}\text{Pb}$.

The sample comes from complex, heterogeneous gneiss of undetermined origin, so it is difficult to determine whether the zircon date represents a period of magmatism or metamorphism. In either case, the zircon date requires that the host gneiss is ca. 1.77 Ga or older, and that either magmatism or metamorphism occurred ca 1.77 Ga.

This zircon age is comparable to those from the Paleoproterozoic arc sequences and plutonic rocks south of the Cheyenne belt exposed in both the Sierra Madre and Medicine Bow Mountains as well as from the Horse Creek region of the Laramie Mountains (see Jones and others, 2010, for summary of existing dates). The arc rocks range in age from ca. 1.780 to 1.771 Ga, with a later pulse of extension-related magmatism ca. 1.763 Ga prior to regional compressional deformation ca. 1.75 Ga (Jones and others, 2010). The biotite gneiss is contemporaneous with the late stages of arc magmatism and may have been deformed either at 1.77 Ga (if the zircons are metamorphic) or during regional compression, ca. 1.75 Ga. The new age matches well with that of the Horse Creek granite (1770 ± 3 Ma) exposed in the Laramie Mountains approximately 80 km (50 mi) to the north (Frost and others, 2000) and with preliminary U-Pb dates of volcanic rocks exposed a few km to the east in the Granite Village area (Houston and Marlatt, 1997; Chamberlain unpublished data).

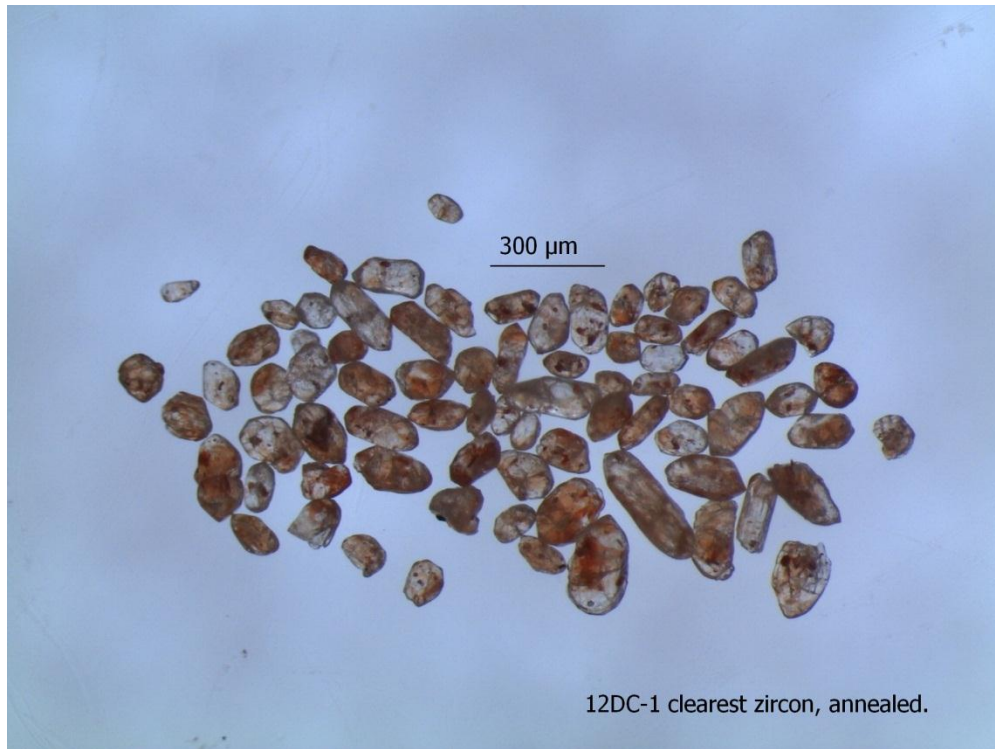


Figure 18. (Top) Zircons selected for annealing and chemical abrasion from sample 12DC-1. Most are iron-stained and cracked with few pristine, clear grains. (Bottom) Examples of partially dissolved zircons after the first step of chemical abrasion, showing the remnant, low-uranium domains. U-Pb data comes from complete dissolution of individual grains of these remnants.

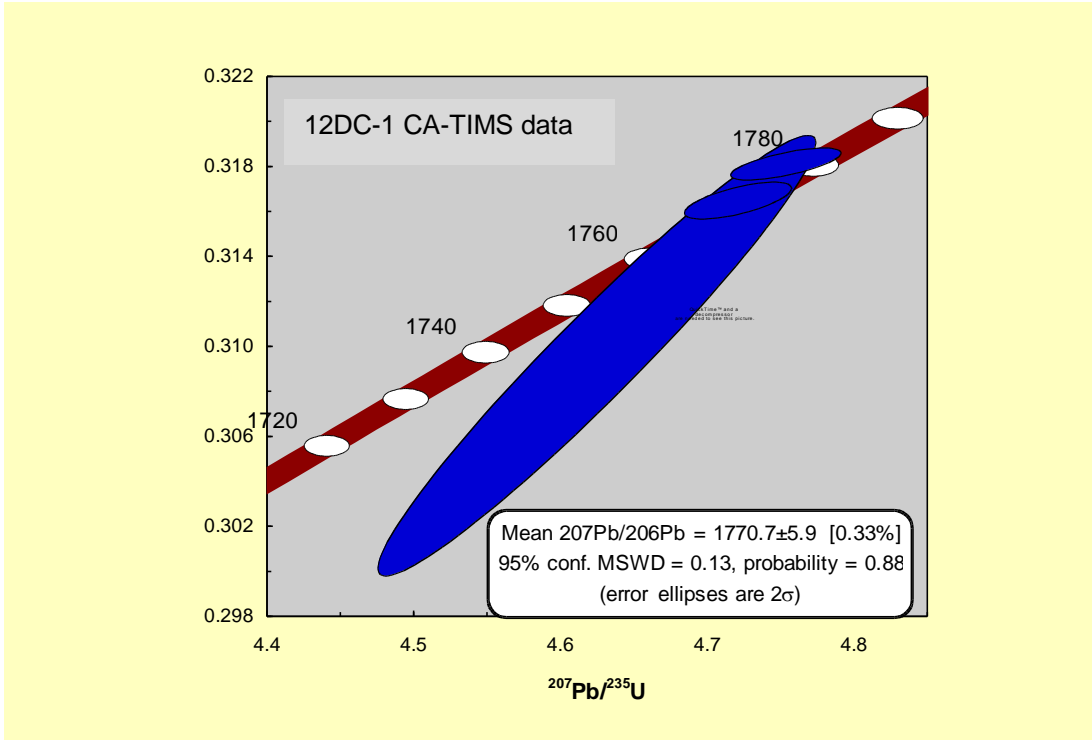


Figure 19. Concordia plot of CA-TIMS U-Pb data from sample 12DC-1.

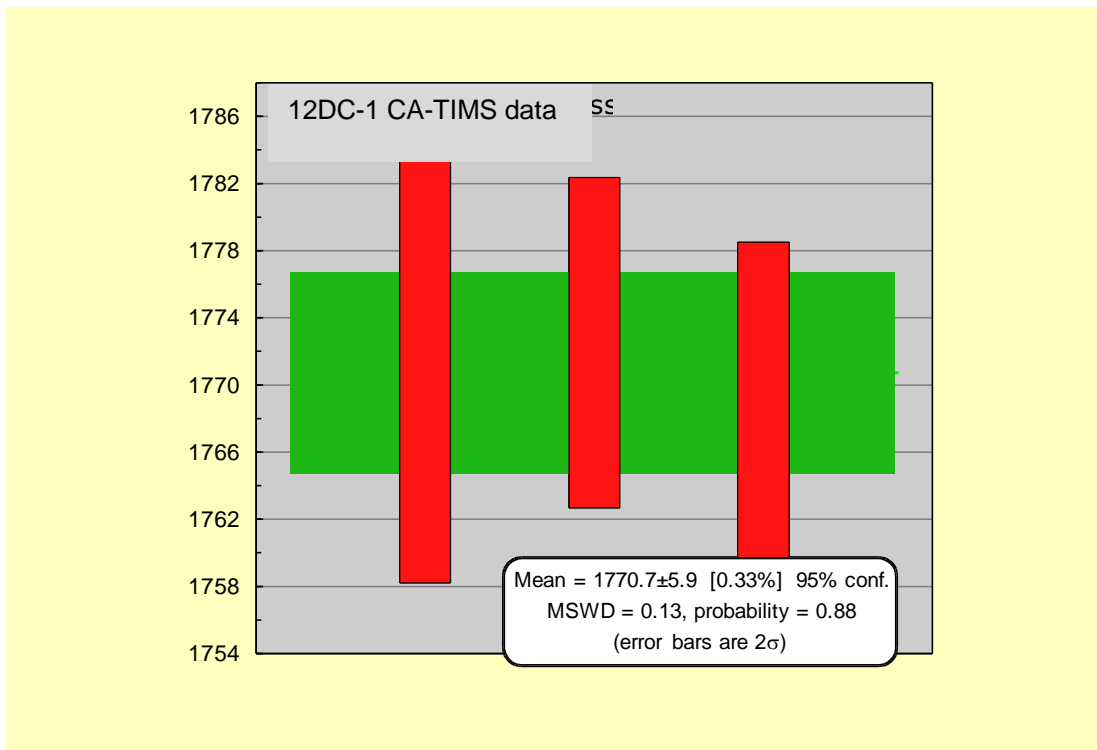


Figure 20. $^{207}\text{Pb}/^{206}\text{Pb}$ dates from sample 12DC-1. The width of the green box represents the uncertainty of the weighted mean date.

Table 3. U-Pb CATIMS zircon data

Sample	Weight (μg)	U (ppm)	sample Pb (pg)	Total Pb (pg)	Corrected atomic ratios										Rho					
					Pb*/ Pbc	$\frac{206\text{Pb}}{204\text{Pb}}$	$\frac{208\text{Pb}}{206\text{Pb}}$	$\frac{206\text{Pb}/238\text{U}}$	$\frac{207\text{Pb}/235\text{U}}$	$\frac{207\text{Pb}/206\text{Pb}}$	$\frac{207\text{Pb}/206\text{Pb}}$	$\frac{206/238 \text{ Age (Ma)}}{\text{Age (Ma)}}$	$\frac{207/235 \text{ Age (Ma)}}{\text{Age (Ma)}}$	$\frac{207/206 \text{ Age (Ma)}}{\text{Age (Ma)}}$		err	% disc.			
12DC-01 Dale Creek (N41.03377 W105.374585)					<i>zircon crystallization age = 1770.7\pm5.9 [0.33%] 95% conf. 3 point weighted 207Pb/206Pb date (MSWD 0.13)</i>															
sC	5.06	101	32	161	1.9	83.8	5265	0.08	0.3097	(2.53)	4.6245	(2.63)	0.1083	(0.70)	1739.3	1753.7	1770.93	\pm 12.7	0.96	2.04
sE	0.90	121	38	35	2.3	15.4	1004	0.05	0.3181	(0.18)	4.7532	(0.65)	0.1084	(0.54)	1780.2	1776.7	1772.46	\pm 9.8	0.69	-0.50
sG	2.16	94	30	65	4.0	16.2	1046	0.06	0.3165	(0.21)	4.7205	(0.63)	0.1082	(0.52)	1772.4	1770.9	1769.04	\pm 9.4	0.67	-0.22

Notes: sample: s = single grain.

Weight: represents estimated weight after first step of CA-TIMS dissolution. U and Pb concentrations are based on these estimates and may be underestimations, depending on how much material was dissolved and leached in the first step.

Picograms (pg) sample and total common Pb from the second dissolution step are measured directly.

sample Pb: sample Pb (radiogenic + initial) corrected for laboratory blank

Total common Pb: all ascribed to laboratory blank.

Pb*/Pbc: radiogenic Pb to total common Pb (blank + initial)

Corrected atomic ratios: $^{206}\text{Pb}/^{204}\text{Pb}$ corrected for mass discrimination and tracer, all others corrected for blank, mass discrimination, and tracer, values in parentheses are 2 sigma errors in percent.

Rho: $^{206}\text{Pb}/^{238}\text{U}$ vs $^{207}\text{Pb}/^{235}\text{U}$ error correlation coefficient

% disc.: percent discordant

Zircon dissolution and chemistry were adapted from methods developed by Krogh (1973), Parrish and others (1987), and Mattinson (2005). All samples were chemically abraded (CA-TIMS) and spiked with a mixed $^{206}\text{Pb}/^{233}\text{U}/^{235}\text{U}$ tracer (ET535). Pb and U samples were loaded onto single rhenium filaments with silica gel.

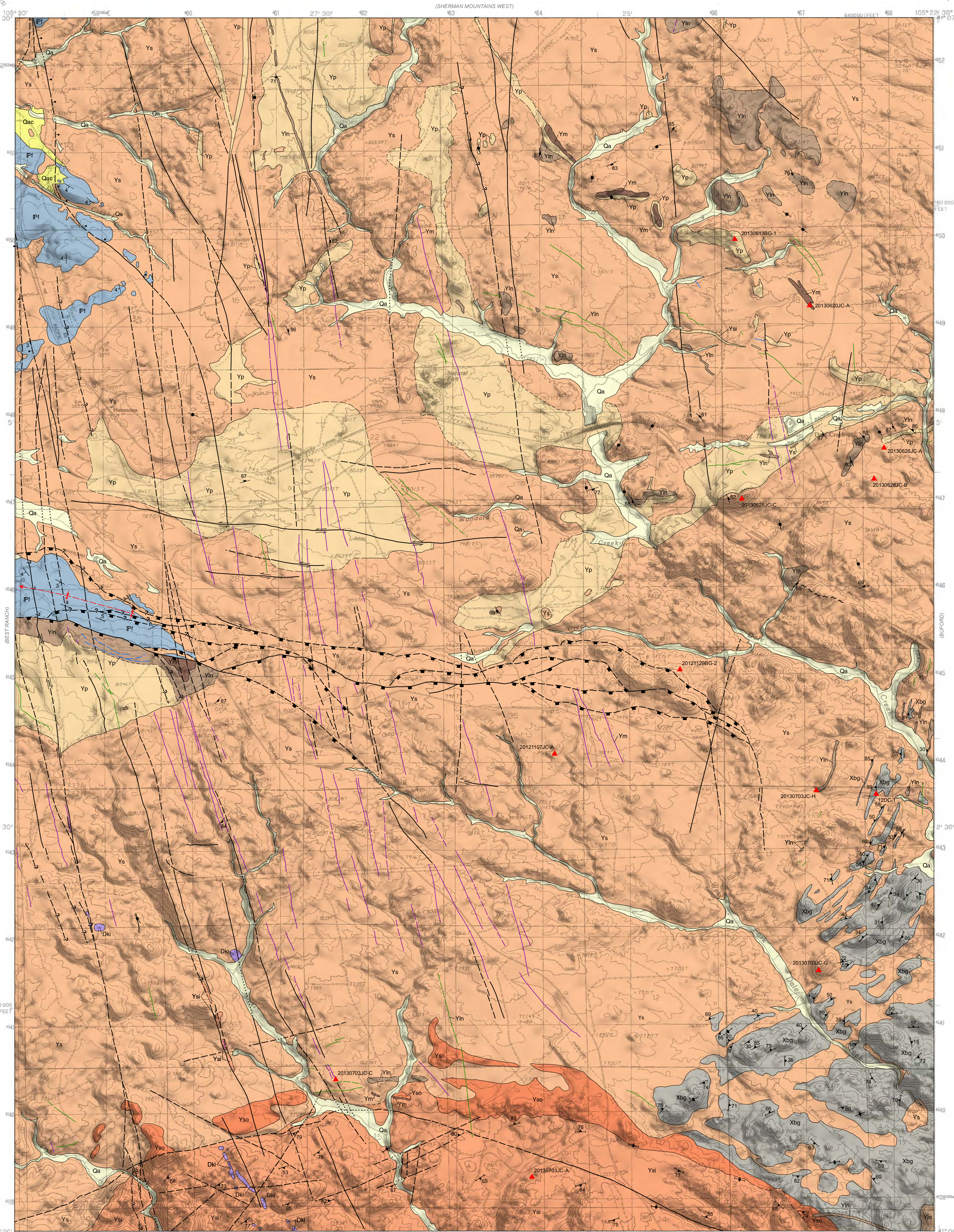
Isotopic compositions were measured in single collector mode on a Micromass Sector 54 mass spectrometer at the University of Wyoming using Daily-photomultiplier for both Pb and UO₂. Mass discrimination of 0.200 ± 0.06 ‰ for Pb was determined by replicate analyses of NIST SRM 981. U fractionation was determined internally.

Isotopic composition of the Pb blank was measured as 18.763 ± 1.2 , 15.675 ± 0.66 , and 38.130 ± 1.88 for 206/204, 207/204 and 208/204, respectively. U blanks were measured at 0.2 pg.

Concordia coordinates, intercepts, and uncertainties were calculated using PBDAT, MacPBDAT and ISOPLOT programs (based on Ludwig 1988, 1991);

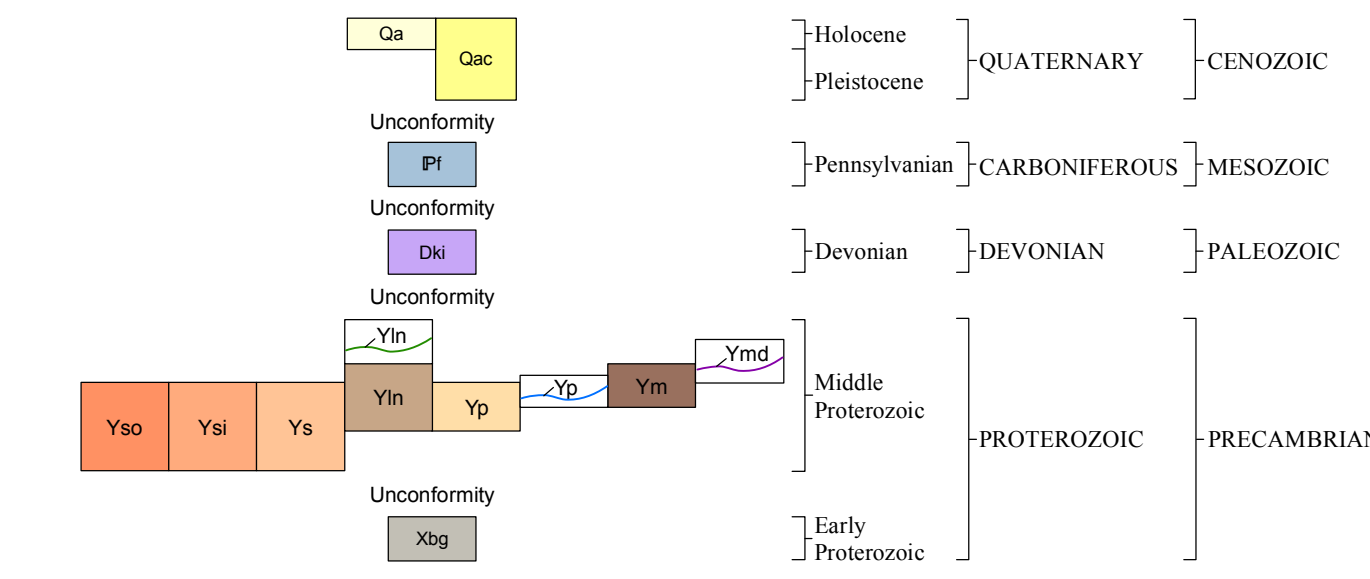
The decay constants used by PBDAT and MacPBDAT are those recommended by the I.U.G.S. Subcommittee on Geochronology (Steiger and Jäger, 1977):

$0.155125 \times 10^9/\text{yr}$ for ^{238}U , $0.98485 \times 10^9/\text{yr}$ for ^{235}U and present-day $^{238}\text{U}/^{235}\text{U} = 137.88$. EARTHTIME spike ET535 has been calibrated against gravimetric standards and tested externally by numerous labs to minimize possible interlaboratory bias.



EXPLANATION

CORRELATION OF MAP UNITS



DESCRIPTION OF MAP UNITS

- Cenozoic**
 - Qa** Alluvium (Holocene)—Unconsolidated to poorly consolidated clay, silt, sand, gravel, cobbles, and boulders, mainly in flood plains and lower stream terraces. Alluvial material is derived from all local geologic units. Thickness approximately 0 to 8 m (25 ft).
 - Qac** Mixed alluvium and colluvium (Holocene and Pleistocene)—Sand, silt, clay, and gravel deposited along intermittent streams; includes slope wash and smaller alluvial fan deposits that coalesce with alluvium. Thickness approximately 0 to 8 m (25 ft).
- Mesozoic**
 - Pf** Fountain Formation (Pennsylvanian)—Coarse-grained pink to red to purple sandstone and arkose, with some conglomerates, fossiliferous limy sandstones, siltstones, shales, and thin limestone lenses. Biotically pink-red iron staining is common on arkosic, resistant, ridge-forming portions of the formation. Thickness is variable within the Laramie Basin (up to 150 m; 500 ft), thickening toward the southwest, but is generally less than 30 m (100 ft) within the map area, representing the lowest part of the formation.
- Paleozoic**
 - Dk** Kimberlitic diatremes (Devonian)—Porphyritic, brecciated, kimberlitic intrusive masses and dikes. Kimberlitic outcrops are subtle but differ from country rock outcrops by their light blue to gray color (blue ground) and often a difference in vegetation—usually grassy, with few, if any trees. Mineral phases include olivine, enstatite, almandine and pyrope garnet, diopside, picroilmenite, and phlogopite; many are diamondiferous; matrix is usually finely crystalline and dominated by serpentine and lesser amounts of carbonate, olivine, perovskite, and phlogopite. Some contain xenoliths of lower Paleozoic sedimentary rocks (Silurian and Ordovician). Mantle-derived nodules of peridotite, eclogite, carbonatite, granulite, and pyroxenite have been found in many Kimberlites of the State Line District (Hause and others, 1979; Hause and Sutherland, 2000).
- Middle Proterozoic**
 - Ym** Lincoln Granite—Medium- to fine-grained, equigranular, orange-red to orange-gray, biotite granite that crops out in horizontal to moderately dipping sheets that tend to cap resistant hills, domes, and high ridges above the Sherman Granite. Some Lincoln Granite occurs as dikes and small inclusions/enclaves in the adjacent Sherman Granite. Major phases include quartz, microcline, plagioclase, perthite, biotite, and hornblende; minor phases include apatite, zircon, ilmenite, magnetite, and myrmekite. Lincoln Granite is generally less abundant than Sherman Granite and is a more evolved phase of the Sherman batholith with relatively high silica content and low iron enrichment. Contacts with the Sherman Granite are generally sharp. Contacts with the porphyritic granite are mingled to sharp. Some samples include isolated alkali feldspar megacrysts that comprise less than 1 percent of the rock (Frost and others, 1999). The Lincoln Granite has been dated at 1,430 ± 2.6 Ma by U-Pb dating (Frost and others, 1999).
 - Ymd** Mafic dike—Mafic dikes cross-cut the Sherman Granite across the entire mapping area, and are most prevalent in the west half of the map. These dikes consist of diabasic to monzodioritic rocks with similar compositions that fall within the range of Mg-rich mafic rocks described by Frost and others (1999). In places, the dikes have diabasic cores that grade into monzodiorite at the dike margins. Minor conchoidal to porphyritic granite is observable. Major phases include plagioclase, biotite, perthite, quartz, and orthoclase; minor phases include apatite, ilmenite, magnetite, zircon, and titanite. Some field samples contain small inclusions of Sherman Granite as well as megacrystic plagioclase that appear to be xenocrysts in thin sections. The mafic dikes are typically oriented parallel to pervasive faults and fractures that trend 340° and 350°. Field relationships suggest dike emplacement during batholith cooling. The mafic dikes have not been directly dated using modern isotope methods. Field relationships as described above suggest a later intrusive age than the Sherman Granite and similar age to Lincoln and porphyritic granites in the range of 1,430 to 1,433 Ma (Edwards, 1993). Some dikes compiled from Hause and others (1981).
 - Yp** Porphyritic granite—Medium-grained, orange-gray to brown biotite hornblende granite with 1 to 4 cm (0.4 to 1.6 in), orange-pink and pink-gray perthitic microcline, and some plagioclase phenocrysts that show rapakivi texture of plagioclase and quartz rims. Major phases include perthitic microcline, plagioclase, quartz, biotite, hornblende; minor phases include ilmenite, apatite, zircon, titanite, and pigeonite. The porphyritic granite crops out as large irregular bodies and as thin dikes that cut the Sherman Granite. Some outcrops of porphyritic granite show orientation of phenocrysts in a single stress direction related to local emplacement deformation. The porphyritic granite (named by Edwards, 1993) is considered a compositional intermediate between the Sherman and Lincoln Granites (Frost and others, 1999). Hematite-rich fluid is evident on crystal faces within the rock and is associated with cross-cutting quartz veins. The porphyritic granite has been dated at 1,430 to 1,433 Ma by modal composition association between the Lincoln and Sherman Granites, respectively (Frost and others, 1999).
- Early Proterozoic**
 - Ys** Main phase—Coarse-grained, pink to reddish-orange, biotite hornblende granite that crops out in rounded to craggy mounds and more commonly a thick weathered crust. Major phases include microcline, plagioclase, quartz, hornblende, biotite, and ilmenite; minor phases include zircon and apatite, and in some locations augite, pigeonite, and fayalite. The Sherman Granite has a subporphyritic granular texture, exhibiting megacrystic microcline rimmed in plagioclase resulting in rapakivi texture in some locations. The main phase of Sherman Granite is the most common phase of the Sherman batholith, and has previously been mapped as the Trail Creek Granite (Eggle, 1968; Hause and others, 1979). Near its contact with Early Proterozoic biotite gneiss, the main phase of the Sherman Granite is medium- to coarse-grained, but the overall texture is similar to that of the main phase elsewhere in the mapping area. The Sherman Granite is a relatively primitive phase of the Sherman batholith with low silica and high iron concentrations. Contacts with both the Lincoln Granite and the porphyritic granite tend to be sharp. Epidote, hematite, and calcium-enrichment associated with hydrothermal alteration are present near its contact with the porphyritic granite and the biotite gneiss. The Sherman Granite has been dated at 1,433 ± 1.5 Ma by U-Pb dating (Frost and others, 1999).
 - Yso** Inner cap rock phase—Pinkish-gray, porphyritic, biotite monzogranite. Foliation defined by oriented, tabular, microcline phenocrysts, biotite-rich streaks, and oriented tabular inclusions (Eggle and Braddock, 1988). Major phases include microcline, plagioclase, quartz, biotite, and magnetite; minor phases include apatite, zircon, allanite, titanite and fluorite (Eggle, 1968). Contact with the outer cap rock phase can be sharp locally, but is generally gradational (Eggle and Braddock, 1988). Contact with the Sherman Granite is sharp.
 - Ysa** Outer cap rock phase—Composition is nearly identical to the inner cap rock, but finer-grained with more abundant biotite streaks and a higher average color index (Eggle, 1968). Phenocrysts are generally smaller than in the inner cap rock phase, but not always present. When present, the phenocrysts can be oriented (Eggle and Braddock, 1988).
- Biotite gneiss—**Gray, pink, or red, medium-grained; composed mostly of quartz, plagioclase, and microcline. Biotite constitutes 10 to 20 percent of rock and occurs as anastomosing seams and elongate, flattened discoid groups that are uniformly distributed. Contacts with adjacent rocks are generally concordant to foliation, but locally discordant (Eggle and Braddock, 1988). Major phases include quartz, plagioclase, microcline, and biotite; minor phases include sparse garnet and opaque oxides. Sample 12DC-1 was dated by U-Pb at 1,771 ± 6 Ma. Sample location noted on map.

MAP SYMBOLS

- Formation contact**—Continuous where certain; long dash where approximate; short dash where inferred; queried where identity or existence uncertain
- Fault**—Continuous where certain; long dash where approximate; short dash where inferred; dotted where concealed; queried where identity or existence uncertain; block on hanging wall of reverse fault; bar and ball on downthrown block (fault type unknown); arrows indicate direction of movement on oblique-slip fault
- Fracture or possible fault**—Continuous where certain; long dash where approximate; short dash where inferred; dotted where concealed; queried where identity or existence uncertain. Sometimes occupied by minor dikes
- Shear zone**—Characterized by brittle deformation and fault breccia; alteration is common
- Syncline**—Long dash where approximate; arrow on end or along axis indicates direction of plunge
- Dike**—Continuous where certain; long dash where approximate
- Lincoln Granite**
- Mafic**
- Porphyritic granite**
- Strike and dip of inclined bedding**
- Strike and dip of joint**
- Strike of vertical joint**
- Strike and dip of foliation**
- Strike of vertical foliation**
- Strike and dip of foliation measurement from Eggle (1968)**
- Strike of vertical foliation measurement from Eggle (1968)**
- Sample location**—Showing sample name (refer to accompanying report for analyses)

MAP REFERENCES

Anderson, J.L., and Callers, R.L., 1999, Paleo- and Mesoproterozoic granite plutonism of Colorado and Wyoming: Rocky Mountain Geology, v. 34, no. 2, p. 149-164.

Blackstone, D.L., Jr., 1996, Structural geology of the Laramie Mountains, southeastern Wyoming and northeastern Colorado: Wyoming State Geological Survey Report of Investigations 51, 28 p.

Edwards, B.R., 1993, A field, geochemical, and isotopic investigation of the igneous rocks in the Pule Mountain area of the Sherman batholith, southern Laramie Mountains, Wyoming, U.S.A.: Laramie, University of Wyoming, M.S. thesis, 164 p., scale 1:24,000.

Edwards, B.R., and Frost, C.D., 2000, An overview of the petrology and geochemistry of the Sherman batholith, southeastern Wyoming—identifying multiple sources of Mesoproterozoic magmatism: Rocky Mountain Geology, v. 35, no. 1, p. 113-137.

Eggle, D.H., 1968, Virginia Dale Precambrian ring-dike complex, Colorado-Wyoming: Geological Society of America Bulletin, v. 79, p. 1545-1564.

Eggle, D.H., and Braddock, W.A., 1988, Geologic map of the Cherokee Park quadrangle, Larimer County, Colorado and Albany County, Wyoming: U.S. Geological Survey Geologic Quadrangle Map GQ-1615, scale 1:24,000.

Eggle, D.H., Larson, E.E., and Bradley, W.C., 1969, Granites, gneisses, and the Sherman erosion surface, southern Laramie Range, Colorado-Wyoming: American Journal of Science, v. 267, p. 510-522.

Ferris, C.S., Jr., and Krueger, H.W., New radiogenic dates on igneous rocks from the southern Laramie Range, Wyoming: Geological Society of America Bulletin, v. 75, p. 1051-1054.

Frost, C.D., and Frost, B.R., 1997, Reduced rapakivi-type granites—The tholeiitic connection: Geology, v. 25, no. 7, p. 647-650.

Frost, C.D., Frost, B.R., Chamberlain, K.R., and Edwards, B.R., 1999, Petrogenesis of the 1.43 Ga Sherman batholith, SE Wyoming, USA—A reduced, rapakivi-type anorogenic granite: Journal of Petrology, v. 40, no. 12, p. 1771-1802.

Hause, W.D., and Sutherland, W.M., 2000, Gemstones and other unique minerals and rocks of Wyoming: Wyoming State Geological Survey Bulletin 71, 268 p.

Hause, W.D., Glahn, P.R., and Woodzick, T.L., 1981, Geological and geophysical investigations of kimberlite in the Laramie Range of southeastern Wyoming: Geological Survey of Wyoming [Wyoming State Geological Survey] Preliminary Report 18, 13 p., 2 pls., scale 1:24,000.

Hause, W.D., McCallum, M.E., and Woodzick, T.L., 1979, Exploration for diamond-bearing kimberlite in Colorado and Wyoming—An evaluation of exploration techniques: Geological Survey of Wyoming [Wyoming State Geological Survey] Report of Investigations 19, 29 p.

Houston, R.S., and Marlatt, G., 1997, Proterozoic geology of the Granite Village area, Albany and Laramie Counties, Wyoming, compared with that of the Sierra Madre and Medicine Bow Mountains of southeastern Wyoming: U.S. Geological Survey Bulletin 2159, 25 p., 1 pl., scale 1:24,000.

Love, J.D., and Christiansen, A.C., 1985, Geologic Map of Wyoming: U.S. Geological Survey, scale 1:500,000.

Love, J.D., and Weitz, J.L., 1953, Geologic map of Albany County, Wyoming: Wyoming Geological Association 8th Annual Field Conference Guidebook, unnumbered map, scale 1:158,400 (also published as an unnumbered map by the Geological Survey of Wyoming [Wyoming State Geological Survey]).

Maughan, E.K., and Wilson, R.F., 1963, Permian and Pennsylvanian strata in southern Wyoming and northern Colorado, in Boland, D.W., and Katch, P.J., eds., Geology of the northern Denver Basin and adjacent uplifts: Rocky Mountain Association of Geologists 14th Field Conference, p. 95-104.

Vasek, R.W., and Kolker, A., 1999, Virginia Dale intrusion, Colorado and Wyoming—Magma-mixing and hybridization in a Proterozoic composite intrusion: Rocky Mountain Geology, v. 34, no. 2, p. 195-222.

Ver Ploeg, A.J., 1999, Reconnaissance/photogeologic map of the Dale Creek quadrangle, Albany County, Wyoming: Wyoming State Geological Survey files (unpublished), scale 1:24,000.

Ver Ploeg, A.J., Bagdonas, D., and McLaughlin, J.F., 2011, Preliminary geologic map of the Best Ranch quadrangle, Albany County, Wyoming: Wyoming State Geological Survey Open File Report 11-7, scale 1:24,000.

Ver Ploeg, A.J., and Boyd, C.S., 2007, Geologic map of the Laramie 30' x 60' quadrangle, Albany and Laramie Counties, southwestern Wyoming: Wyoming State Geological Survey Map Series 77, scale 1:100,000.

Ver Ploeg, A.J., and McLaughlin, J.F., 2010, Preliminary geologic map of the Sherman Mountains West quadrangle: Wyoming State Geological Survey Open File Report 10-3, scale 1:24,000.

Zielinski, R.A., Peterman, Z.E., Stuckless, J.S., Rosholt, J.N., and Nkomo, I.T., 1981, The chemical and isotopic record of rock-water interaction in the Sherman Granite, Wyoming and Colorado: Contributions to Mineralogy and Petrology, v. 78, p. 209-291.

DISCLAIMERS

Users of these maps are cautioned against using the data at scales different from those at which the maps were compiled. Using these data at a larger scale will not provide greater accuracy and is, in fact, a misuse of the data.

The Wyoming State Geological Survey (WSGS) and the State of Wyoming make no representation or warranty, expressed or implied, regarding the use, accuracy, or completeness of the data presented herein, or of a map printed from these data. The act of distribution shall not constitute such a warranty. The WSGS does not guarantee the digital data or any map printed from the data to be free of errors or inaccuracies.

The WSGS and the State of Wyoming disclaim any responsibility or liability for interpretations made from these digital data or from any map printed from these digital data, and for any decisions based on the digital data or printed maps. The WSGS and the State of Wyoming retain and do not waive sovereign immunity.

The use of reference to trademarks, trade names, and other product or company names in this publication is for descriptive or informational purposes only, and is pursuant to licensing agreements between the WSGS or State of Wyoming and software or hardware developers/vendors, and does not imply endorsement of those products by the WSGS or the State of Wyoming.

NOTICE TO USERS OF INFORMATION FROM THE WYOMING STATE GEOLOGICAL SURVEY

The WSGS encourages the fair use of its material. We request that credit be expressly given to the "Wyoming State Geological Survey" when citing information from this publication. Please contact the WSGS at 307-766-2286, ext. 224, or by email at wsgs.sales@wyo.gov if you have questions about citing materials, preparing acknowledgments, or extensive use of this material. We appreciate your cooperation.

Individuals with disabilities who require an alternative form of this publication should contact the WSGS. For the TTY relay operator call 800-877-9975.

For more information about the WSGS or to order publications and maps, go to www.wsgs.wyo.edu, call 307-766-2286, ext. 224, or email wsgs.sales@wyo.gov.

NOTICE FOR OPEN FILE REPORTS PUBLISHED BY THE WGS

This WSGS Open File Report has not been technically reviewed or edited for conformity with WSGS standards or Federal Geographic Data Committee digital cartographic standards. Open File Reports are preliminary and usually require additional fieldwork and/or compilation and analysis; they are meant to be a first release of information for public comment and review. The WSGS welcomes any comments, suggestions, and contributions from users of the information.

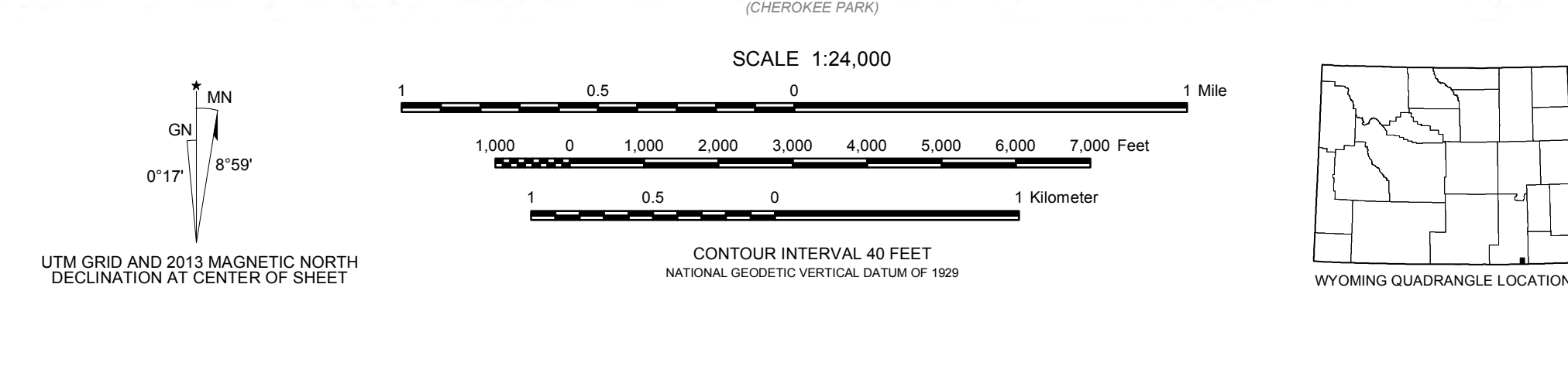
Base map from U.S. Geological Survey 1:24,000 - scale topographic map of the Dale Creek, Wyoming Quadrangle, provisional edition, 1987

Base hillshade derived from USGS/ANRCS - National Cartography & Geospatial Center 10-meter Digital Elevation Model (DEM), 2000, azimuth 035°, sun angle 45°, vertical exaggeration 1.4

Projection: Universal Transverse Mercator (UTM), zone 13 North American Datum of 1987 (NAD 27) 1,000-meter grid ticks: UTM, zone 13 10,000-foot grid ticks: Wyoming State Plane Coordinate System, east zone

Wyoming State Geological Survey
P.O. Box 1347 - Laramie, WY 82073-1347
Phone: 307-766-2286 - Fax: 307-766-2605
Email: wsgs.sales@wyo.gov

A digital version of this map is also available on CD-ROM



Digital cartography by Ranie M. Lynds and Jacob D. Carnes

Map edited by Suzanne C. Lühr

Prepared in cooperation with and research supported by the U.S. Geological Survey, National Cooperative Geologic Mapping Program, under USGS award number G12AC29465. The views and conclusions contained in this document are those of the authors and should not be interpreted as necessarily representing the official policies, either expressed or implied, of the U.S. Government.

PRELIMINARY GEOLOGIC MAP OF THE DALE CREEK QUADRANGLE, ALBANY COUNTY, WYOMING

by
Jacob D. Carnes, Ranie M. Lynds, Robert W. Gregory, and Alan J. Ver Ploeg